(1953).

[10]N. Kurti, Nuovo Cimento Suppl. VI, Serie X, 1101 (1957).

[11]H. Lipson, C. A. Beevers, Proc. Roy. Soc. A148, 664 (1935); and Proc. Roy. Soc. A151, 347 (1935).

[12]D. Schiferl, J. Chem. Phys. 52, 3234 (1970).

[13]S. Haussuhl, Z. Kristallogr. 116, 371 (1961).

[14]W. Hofmann, Z. Kristallogr. 78, 279 (1931).

[15]B. Bleaney and K. W. H. Stevens, Rep. Prog. Phys. 16, 108 (1953).

[16]K. D. Bowers and J. Owen, Rep. Prog. Phys. 18, 304 (1955).

[17]J. H. Van Vleck, Revista Tucuman, 14, 189 (1961).

[18]J. Hori, *Spectral Properties of Disordered Chains and Lattices* (Pergamon, New York, 1968).

[19]H. A. Farach, C. P. Poole, Jr., and J. M. Daniels, Phys. Rev. 188, 864 (1969).

[20]M. H. Cohen and F. Keffer, Phys. Rev. 99, 1128 (1955).

[21]R. P. Hudson, *American Institute of Physics Handbook*, edited by D. G. Gray (McGraw-Hill, New York, 1972).

[22]P. H. E. Meijer, Phys. Rev. B 3, 182 (1971).

[23]R. J. Benzie and A. H. Cooke, Proc. Roy. Soc. A209, 269 (1951).

[24]N. Kurti, P. Laine, and F. Simon, Compt. Rend. 204, 675 (1937).

[25]R. J. Benzie, A. H. Cooke, and S. Whitley, Proc. Roy. Soc. A232, 277 (1955).

[26]D. M. S. Bagguley and J. H. E. Griffiths, Nature

162, 538 (1948).

[27]B. Bleaney, R. P. Penrose, and B. I. Plumpton, Proc. Roy. Soc. A198, 406 (1949).

[28]B. W. Mangum (unpublished).

[29]J. M. Daniels and F. N. H. Robinson, Phil. Mag. 44, 630 (1953).

[30]A. H. Cooke, H. J. Duffus, and W. P. Wolf, 44, 623 (1953).

[31]K. W. Mess, H. Lubbers, L. Niesen, and W. J. Huiskamp, Physica 41, 260 (1969).

[32]K. W. Mess, L. Niesen, and W. J. Huiskamp, Physica 45, 626 (1970).

[33]G. O. Zimmerman, D. J. Abeshouse, E. Maxwell, and D. R. Kelland, Physica 51, 623 (1971).

[34]D. Abeshouse, thesis (Boston University, 1971) (unpublished).

[35]S. Wang, S. T. Dembinski, and W. Opechowski, Physica 42, 565 (1969).

[36]R. P. Hudson and E. Pfeiffer (unpublished).

[37]R. Finkelstein and A. Mencher, J. Chem. Phys. 21, 472 (1953).

[38]C. E. Johnson and H. Meyer, Proc. Roy. Soc. (London) A253, 199 (1959).

[39]A. H. Cooke, H. Meyer, and W. P. Wolf, Proc. Roy. Soc. A233, 536 (1956).

[40]H. Meyer, Phil. Mag. 8, 2, 521 (1957).

[41]J. M. Baker, Phys. Rev. 136, A1341 (1964).

[42]J. A. Ketelaar, Physica 4, 619 (1937).

Electronic-Structure Studies of Solids. II. "Exact" Hartree–Fock Calculations for Cubic Atomic-Hydrogen Crystals*

Frank E. Harris, Lalit Kumar, and Hendrik J. Monkhorst

Department of Physics, University of Utah, Salt Lake City, Utah 84112

(Received 5 September 1972)

A comprehensive description is given of rigorous Hartree–Fock calculations for cubic atomic-hydrogen crystals. All energy and overlap integrals are reduced to reciprocal-lattice sums. The exchange effects are treated exactly. The Bloch functions and Fermi surfaces are optimized. The near-Hartree–Fock results indicate essentially spherical Fermi surfaces and strong atomic-orbital behavior of the Bloch functions. The energetic effect associated with the atomlike inhomogeneities is about 15%. Good agreement is found between Kohn–Sham and Slater local-exchange potentials and exchange potentials deduced from our Hartree–Fock results.

I. INTRODUCTION

Modern band theory has had generally great success in describing the electronic properties of solids. Different approximation schemes have been developed, and their ranges of validity are quite well understood.[1] However, all these methods have in common the use of one-particle crystal potentials in Schrödinger-type equations for the band functions. Perhaps most seriously, the exchange and correlation effects are described by local potentials, and parametrization of the theory

is hampered by nontransferability of the parameters.[2] Nevertheless, band theory has given considerable insight into the properties of a large number of crystals of varying complexities.[3]

It would be highly desirable to have accurate Hartree–Fock results for at least some representative crystals. Such results might be of assistance in the choice of optimum basis orbitals and exchange potentials, and might help in the systematic inclusion of correlation effects. Hartree–Fock results would also enable the definitive evaluation of exchange and correlation effects upon the cohe-

sive energy and the magnetic and electric proper-
ties of crystalline solids.

Recently we have proposed a formulation for the
exact solution of the Hartree–Fock problem for
crystals.[4] We introduced Fourier-transform for-
mulas for the crystal integrals, and showed how a
systematic exploitation of lattice orthogonality
relations entirely eliminates the multicenter inte-
gral problem usually encountered in conventional
all-electron calculations. The formulation there-
fore involves reciprocal-lattice summations re-
quiring Fourier transforms of basis atomic orbitals
only. The exchange contribution is evaluated ex-
actly, and we arrive at a natural and precise un-
derstanding of the cancellation of long-range con-
tributions to the electrostatic energy. We have ob-
served a far more rapid convergence than may
have been expected.[5]

In the first paper of this series[6] (hereafter re-
ferred to as I) we have applied the Fourier-repre-
sentation method to the Madelung problem. Veri-
fying known Madelung constants, we showed the
mathematical and numerical steps to be correct
and useful. We also calculated lattice-structure
constants as they appear both in the Madelung
problem and in our Hartree–Fock formulation.
Reports on numerical aspects and results for dif-
ferent atomic-hydrogen crystals have appeared
recently.[5,7]

We now wish to present a more complete account
of the formalism, numerical techniques, and re-
sults of Hartree–Fock calculations for the simple-
cubic (sc), body-centered-cubic (bcc), and face-
centered-cubic (fcc) atomic-hydrogen crystals. In
Secs. II–VI we describe the theory, working for-
mulas, and numerical techniques. The organiza-
tion of the computer programs is briefly sketched.
Sections VII and VIII comprise the results and their
analysis. It is indicated that we have reached a
near-Hartree–Fock limit, with Hartree–Fock
Bloch orbitals that exhibit considerable atomic-
orbital behavior. Remarkable agreement is found
between local-exchange potentials and potentials
derived from the exact exchange operator as found
in our work.

II. FORMULATION OF PROBLEM

Consider a cubic lattice of hydrogen atoms at
0 °K, with a proton fixed at each lattice site and an
equal number of electrons distributed through the
crystal. The electrons are assumed to doubly oc-
cupy Bloch functions constructed from atomic or-
bitals. The lattice is considered to be built up
from N cubic unit cells with sides a. The number
of atoms per unit cell is denoted by d, and their
position vectors relative to the cell origin are $a\vec{s}_m$
$(m = 1, \ldots, d)$, with $\vec{s}_1 = 0$. The d values and $\vec{s}$ vec-
tors for sc, bcc, and fcc structures, along with

other quantities, have been summarized in Table I.

The Bloch functions $|\vec{k}\rangle$ are assumed to take the
form

$$|\vec{k}\rangle = \sum_{i=1}^{M} c_i(\vec{k})|\vec{k}_i\rangle , \tag{1}$$

$$|\vec{k}_i\rangle = e^{2\pi i a^{-1}\vec{k}\cdot\vec{r}}\sum_{\vec{\mu}} \Phi_i(\vec{r} - a\vec{\mu}) , \tag{2}$$

$$\Phi_i(\vec{r}) = \sum_{m=1}^{d} \phi_i(\vec{r} - a\vec{s}_m) . \tag{3}$$

In Eq. (1) the summation is over basis Bloch or-
bitals $|\vec{k}_i\rangle$ defined by Eqs. (2) and (3). Additional
$\vec{k}$ dependence is introduced through the expansion
coefficients in $|\vec{k}\rangle$. In Eq. (2) the sum is over N
compound-unit-cell basis functions Φ_i which in
turn are the sum of the basis atomic orbitals ϕ_i
centered at the nuclear positions $a\vec{s}_m$ in the com-
pound cell [Eq. (3)]. Vectors designated by Greek
letters, such as $\vec{\mu}$, refer to the origin of a unit
cell; in the unit system used here the components
of such vectors are integers and $\vec{k}$ is dimensionless.
A prime on a Greek vector summation will be used
to indicate that the origin point is to be omitted.
The $|\vec{k}_i\rangle$ differ from our initial work,[4] and may be
regarded as modulated plane waves rather than as
conventional tight-binding Bloch orbitals. Any
inadequacy in the $\vec{k}$ dependence of the $|\vec{k}_i\rangle$ can be
corrected through the $\vec{k}$ dependence of the coeffi-
cients $c_i(\vec{k})$.

The nonrelativistic Hamiltonian H can be cast in
the form (in atomic units)

$$H = \sum_{i=1}^{Nd} (-\tfrac{1}{2}\nabla_i^2) + \sum_{1\leq i\leq j\leq Nd} h(\vec{r}_i, \vec{r}_j) , \tag{4}$$

$$h(\vec{r}_1, \vec{r}_2) = r_{12}^{-1} - \frac{1}{Nd}\sum_{\vec{\mu}}\sum_{m=1}^{d} |\vec{r}_1 - a\vec{\mu} - a\vec{s}_m|^{-1}$$

$$- \frac{1}{Nd}\sum_{\vec{\mu}'}\sum_{m'=1}^{d} |\vec{r}_2 - a\vec{\mu}' - a\vec{s}_{m'}|^{-1}$$

$$+ \frac{1}{N^2 da}\left(\sum_{\vec{\mu}\neq\vec{\mu}'} |\vec{\mu} - \vec{\mu}'|^{-1} + \sum_{m=2}^{d} |\vec{\mu} - \vec{\mu}' - \vec{s}_m|^{-1}\right) . \tag{5}$$

The Hamiltonian of Eq. (4) is exact except for
terms which are of order less than N. The last

TABLE I. Parameters for cubic atomic-hydrogen
crystals.[a]

Lattice	d	$\vec{s}_m$	V_{FS}	D
sc	1	$(0,0,0)$	$\tfrac{1}{2}$	-8.913633
bcc	2	$(0,0,0); (\tfrac{1}{2},\tfrac{1}{2},\tfrac{1}{2})$	1	-11.432989
fcc	4	$(0,0,0); (\tfrac{1}{2},0,\tfrac{1}{2}) (\tfrac{1}{2},\tfrac{1}{2},0); (0,\tfrac{1}{2},\tfrac{1}{2})$	2	-14.403769

[a]d is the number of atoms per compound cell (cubic, of
linear dimension a). $\vec{s}_m$ are position vectors (in units a)
of atoms in compound cell relative to its origin $(n=1\ldots,d)$;
V_{FS} is the volume in reciprocal space enclosed by the
Fermi surface, in units $(2\pi/a)^3$; D is the lattice-structure
constant as defined in Eq. (29).

summation of Eq. (5) should be omitted if $d = 1$ (simple-cubic case). With the assumption of double occupancy of the crystal wave functions and the antisymmetry requirement of the Bloch orbitals, the expectation value of the energy takes the form

$$E = 2N \int d\vec{k} \, \frac{\langle \vec{k} | - \frac{1}{2}\nabla^2 | \vec{k} \rangle}{\langle \vec{k} | \vec{k} \rangle}$$
$$+ 2N^2 \int d\vec{k} \, d\vec{k}' \, \frac{\langle \vec{k}\vec{k}' | h | \vec{k}\vec{k}' \rangle - \frac{1}{2}\langle \vec{k}\vec{k}' | r_{12}^{-1} | \vec{k}'\vec{k} \rangle}{\langle \vec{k} | \vec{k} \rangle \langle \vec{k}' | \vec{k}' \rangle} \, . \quad (6)$$

In Eq. (6), and for the remainder of this paper, the integrals of $\vec{k}$ and $\vec{k}'$ are over the reciprocal-lattice space enclosed by the Fermi surface, with volume $\frac{1}{2}d$ in units $(2\pi/a)^3$. The Bloch orbitals can be scaled according to

$$\langle \vec{k} | \vec{k} \rangle = \sum_{i,j=1}^{M} c_i^*(\vec{k})\langle \vec{k}_i | \vec{k}_j \rangle c_j(\vec{k}) = Nd \, . \quad (7)$$

With Eq. (7) the total energy reduces to

$$E = \frac{2}{d} \int d\vec{k} \sum_{ij} c_i^*(\vec{k})\langle \vec{k}_i | - \frac{1}{2}\nabla^2 | \vec{k}_j \rangle c_j(\vec{k})$$
$$+ \frac{2}{d^2} \int d\vec{k} \, d\vec{k}' \sum_{ijmn} c_i^*(\vec{k})c_j(\vec{k})c_m^*(\vec{k}')c_n(\vec{k}')$$
$$\times (\langle \vec{k}_i\vec{k}_m' | h | \vec{k}_j\vec{k}_n' \rangle - \frac{1}{2}\langle \vec{k}_i\vec{k}_m' | r_{12}^{-1} | \vec{k}_n'\vec{k}_j \rangle) \, . \quad (8)$$

The Hartree–Fock equations are now obtained by minimizing E by variation of the $c_i(\vec{k})$ and the form of the Fermi surface, subject to the scaling restrictions of Eq. (7) and to the requirement that the Fermi surface enclose a volume $\frac{1}{2}d$. Using Lagrangian-multiplier methods, we consider the variation $\delta[E - (2/d)\int d\vec{k}\,\epsilon(\vec{k})\langle \vec{k}|\vec{k}\rangle]$, with $\epsilon(\vec{k})$ the Lagrangian multiplier. The result is

$$\sum_j F_{ij}(\vec{k})c_j(\vec{k}) = \epsilon(\vec{k})\sum_j S_{ij}c_j(\vec{k}) \, , \quad (9)$$

$$F_{ij}(\vec{k}) = \left(\frac{1}{Nd}\right)\left[\langle \vec{k}_i | - \frac{1}{2}\nabla^2 | \vec{k}_j \rangle + \left(\frac{2}{d}\right)\sum_{mn}\int d\vec{k}' \right.$$
$$\times c_m^*(\vec{k}')c_n(\vec{k}')(\langle \vec{k}_i\vec{k}_m' | h | \vec{k}_j\vec{k}_n' \rangle$$
$$\left. - \frac{1}{2}\langle \vec{k}_i\vec{k}_m' | r_{12}^{-1} | \vec{k}_n'\vec{k}_j \rangle) \right] \, , \quad (10)$$

$$S_{ij} = (1/Nd)\langle \vec{k}_i | \vec{k}_j \rangle \, , \quad (11)$$

$$\epsilon(\vec{k}_F) = \text{const}, \quad \vec{k}_F \text{ on the Fermi surface.} \quad (12)$$

Equation (12) corresponds to Koopman's theorem but it is here exact because of the continuous variations in $\vec{k}$ as N approaches infinity.

III. MATRIX ELEMENTS

We now reduce the matrix elements appearing in Eqs. (9)–(11). Using the Fourier-representation method, we express these quantities using Fourier transforms of lattice sums of orbital products:

$$\Phi_{ij}(\vec{q}) = \sum_{\vec{\mu}} \langle \Phi_i(\vec{r}) | e^{2\pi i a^{-1}\vec{q}\cdot\vec{r}} | \Phi_j(\vec{r} - a\vec{\mu}) \rangle \, , \quad (13)$$

where the transform variable $\vec{q}$ is in dimensionless units. The overlap integrals can now be reduced to

$$\langle \vec{k}_i | \vec{k}_j \rangle = \sum_{\vec{\lambda},\vec{\mu}} \langle e^{2\pi i a^{-1}\vec{k}\cdot\vec{r}}\Phi_i(\vec{r} - a\vec{\mu}) | e^{2\pi i a^{-1}\vec{k}\cdot\vec{r}}\Phi_j(\vec{r} - a\vec{\lambda}) \rangle$$
$$= N\sum_{\vec{\mu}} \langle \Phi_i(\vec{r}) | \Phi_j(\vec{r} - a\vec{\mu}) \rangle = N\Phi_{ij}(0) \, . \quad (14)$$

Thus S_{ij} satisfies

$$S_{ij} = (1/d)\Phi_{ij}(0) \, . \quad (15)$$

The kinetic-energy integrals involve a form more general than $\Phi_{ij}(\vec{q})$. Writing

$$-\frac{1}{2}\nabla^2 | \vec{k}_j \rangle = e^{2\pi i a^{-1}\vec{k}\cdot\vec{r}}\sum_{\vec{\mu}} (-\frac{1}{2}\nabla^2)\Phi_j(\vec{r} - a\vec{\mu}) + \frac{2\pi^2 k^2}{a^2} | \vec{k}_j \rangle$$
$$-\left(\frac{2\pi i}{a}\right)e^{2\pi i a^{-1}\vec{k}\cdot\vec{r}}\sum_{\vec{\mu}} \vec{k}\cdot\vec{\nabla}\Phi_j(\vec{r} - a\vec{\mu}) \, , \quad (16)$$

we find

$$\langle \vec{k}_i | - \frac{1}{2}\nabla^2 | \vec{k}_j \rangle = N\left(T_{ij} + \frac{2\pi^2 k^2}{a^2} S_{ij}\right) \, , \quad (17)$$

$$T_{ij} = (1/d)\langle \Phi_i(\vec{r}) | - \frac{1}{2}\nabla^2 | \Phi_j(\vec{r} - a\vec{\mu}) \rangle \, . \quad (18)$$

The last term in Eq. (16) gives no contributions as its summation is antisymmetric in $\vec{r}$.

Next we reduce the matrix elements of h to reciprocal-lattice summations. This is done by the aid of Fourier representations of the one- and two-electron integrals.[8] First the r_{12}^{-1} integral is cast into the form

$$\langle \vec{k}_i\vec{k}_m' | r_{12}^{-1} | \vec{k}_j\vec{k}_n' \rangle = \sum_{\vec{\lambda}\vec{\lambda}'\vec{\mu}\vec{\mu}'} \langle \Phi_i(\vec{r}_1 - a\vec{\lambda})\Phi_m(\vec{r}_2 - a\vec{\lambda}') | r_{12}^{-1} | \Phi_j(\vec{r}_1 - a\vec{\mu})\Phi_n(\vec{r}_2 - a\vec{\mu}') \rangle$$

$$= \frac{1}{\pi a} \int \frac{d\vec{q}}{q^2} \sum_{\vec{\lambda}\vec{\lambda}'} e^{-2\pi i\vec{q}\cdot(\vec{\lambda}-\vec{\lambda}')} \sum_{\vec{\mu}} [\Phi_i^*(\vec{r}_1)\Phi_j(\vec{r}_1 - a\vec{\mu} + a\vec{\lambda})]^T(\vec{q}) \sum_{\vec{\mu}'} [\Phi_m^*(\vec{r}_2)\Phi_n(\vec{r}_2 - a\vec{\mu}' + a\vec{\lambda}')]^T(-\vec{q})$$

$$= \frac{1}{\pi a} \int \frac{d\vec{q}}{q^2} \sum_{\vec{\lambda}\vec{\lambda}'} e^{-2\pi i\vec{q}\cdot(\vec{\lambda}-\vec{\lambda}')}\Phi_{ij}(\vec{q})\Phi_{mn}(-\vec{q}) \, . \quad (19)$$

Here and henceforth the superscript T denotes Fourier transform. The last identity holds since the summations over $\vec{\mu}$ and $\vec{\mu}'$ are independent of $\vec{\lambda}$ and $\vec{\lambda}'$, respectively. We then invoke the lattice-orthogonality relation

$$\sum_{\vec{\lambda}\vec{\lambda}'} e^{-2\pi i\vec{q}\cdot(\vec{\lambda}-\vec{\lambda}')} = N\sum_{\vec{\nu}} \delta(\vec{q} - \vec{\nu}) \, , \quad (20)$$

where $\delta(\vec{q})$ is the Dirac δ function. Temporarily ignoring any questions arising from the singularity at $\vec{\nu}=0$, Eq. (19) reduces to

$$\langle \vec{k}_i \vec{k}_m' | r_{12}^{-1} | \vec{k}_j \vec{k}_n' \rangle = \frac{N}{\pi a} \sum_{\vec{\nu}} \nu^{-2} \Phi_{ij}(\vec{\nu}) \Phi_{mn}(-\vec{\nu}) . \quad (21)$$

Using similar Fourier representations, the one-electron terms of h reduce as follows:

$$\langle \vec{k}_i \vec{k}_m' | \frac{1}{Nd} \sum_{\vec{\mu}} \sum_{l=1}^{d} |\vec{r}_1 - a\vec{\mu} - a\vec{s}_l|^{-1} | \vec{k}_j \vec{k}_n' \rangle$$

$$= \frac{1}{\pi d a} \int \frac{d\vec{q}}{q^2} \sum_{\vec{\lambda}\vec{\mu}} e^{-2\pi i \vec{q} \cdot (\vec{\lambda}-\vec{\mu})} \sum_{l=1}^{d} e^{+2\pi i \vec{q} \cdot \vec{s}_l} \Phi_{ij}(\vec{q}) \Phi_{mn}(0) , \quad (22)$$

where $\langle \vec{k}_m' | \vec{k}_n' \rangle$ has been replaced by $N\Phi_{mn}(0)$. If we now define the structure factor $S(\vec{q})$ as

$$S(\vec{q}) = \sum_{m=1}^{d} e^{2\pi i \vec{q} \cdot \vec{s}_m} \quad (23)$$

and again apply Eq. (20), we obtain

$$\langle \vec{k}_i \vec{k}_m' | \frac{1}{Nd} \sum_{\vec{\mu}} \sum_{l=1}^{d} |\vec{r}_1 - a\vec{\mu} - a\vec{s}_l|^{-1} | \vec{k}_j \vec{k}_n' \rangle$$

$$= \frac{N}{\pi d a} \sum_{\vec{\nu}} \nu^{-2} S(\vec{\nu}) \Phi_{ij}(\vec{\nu}) \Phi_{mn}(0) \quad (24)$$

Similarly,

$$\langle \vec{k}_i \vec{k}_m' | \frac{1}{Nd} \sum_{\vec{\mu}'} \sum_{l'=1}^{\phi} |\vec{r}_2 - a\vec{\mu}' - a\vec{s}_{l'}|^{-1} | \vec{k}_j \vec{k}_n' \rangle$$

$$= \frac{N}{\pi d a} \sum_{\vec{\nu}} \nu^{-2} \Phi_{ij}(0) \Phi_{mn}(-\vec{\nu}) S(-\vec{\nu}) . \quad (25)$$

Again we ignore the singularities at $\vec{\nu}=0$.

The last term of h is handled by introduction of the Fourier representation of the inverse distances:

$$\langle \vec{k}_i \vec{k}_m' | \frac{1}{N^2 da} \left(\sum_{\vec{\mu} \neq \vec{\mu}'} |\vec{\mu} - \vec{\mu}'|^{-1} \right.$$

$$\left. + \sum_{\vec{\mu}, \vec{\mu}'} \sum_{l=2}^{d} |\vec{\mu} - \vec{\mu}' - \vec{s}_l|^{-1} \right) | \vec{k}_j \vec{k}_n' \rangle$$

$$= \frac{1}{\pi d a} \frac{d\vec{q}}{q^2} \left(\sum_{\vec{\mu} \neq \vec{\mu}'} e^{-2\pi i \vec{q} \cdot (\vec{\mu}-\vec{\mu}')} \right.$$

$$\left. + \sum_{\vec{\mu}, \vec{\mu}'} \sum_{l=2}^{d} e^{-2\pi i \vec{q} \cdot (\vec{\mu}-\vec{\mu}'-\vec{s}_l)} \right) \Phi_{ij}(0) \Phi_{mn}(0)$$

$$= \frac{1}{\pi d a} \int \frac{d\vec{q}}{q^2} \left(\sum_{\vec{\mu}, \vec{\mu}'} e^{-2\pi i \vec{q} \cdot (\vec{\mu}-\vec{\mu}')} S(\vec{q}) - N \right) \Phi_{ij}(0) \Phi_{mn}(0) . \quad (26)$$

The last identity is obtained by adding and subtracting the terms with $\vec{\mu} = \vec{\mu}'$. Once again we invoke Eq. (20), ignoring singularities at $\vec{\nu}=0$ and $\vec{q}=0$, reaching

$$\langle \vec{k}_i \vec{k}_m' | \frac{1}{N^2 da} \left(\sum_{\vec{\mu} \neq \vec{\mu}'} |\vec{\mu} - \vec{\mu}'|^{-1} \right.$$

$$\left. + \sum_{\vec{\mu}\vec{\mu}'} \sum_{l=2}^{d} |\vec{\mu} - \vec{\mu}' - \vec{s}_l|^{-1} \right) | \vec{k}_j \vec{k}_n' \rangle$$

$$= \frac{N}{\pi d a} \left(\sum_{\vec{\nu}} \nu^{-2} S(\vec{\nu}) - \int \frac{d\vec{q}}{q^2} \right) \Phi_{ij}(0) \Phi_{mn}(0) . \quad (27)$$

We now have to discuss the $\vec{\nu}=0$ and $\vec{q}=0$ singularities ignored in deriving Eqs. (21), (24), (25), and (27). It is shown in Appendix A of I that these singularities arise from the interchange of the summation of Eq. (20) with the $\vec{q}$ integration in a region near $\vec{q}=0$ where the uniform convergence needed to justify the interchange is lacking. It is also shown that a more careful analysis leads to the conclusion that a correct result is obtained if the $\vec{\nu}=0$ terms are dropped from all summations in Eqs. (21), (24), (25), and (27). We then obtain

$$\langle \vec{k}_i \vec{k}_m' | h | \vec{k}_j \vec{k}_n' \rangle = \frac{N}{\pi a} \sum_{\vec{\nu}} {}' \nu^{-2} \left(\Phi_{ij}(\vec{\nu}) \Phi_{mn}(-\vec{\nu}) \right.$$

$$- \frac{S(\vec{\nu})}{d} \Phi_{ij}(\vec{\nu}) \Phi_{mn}(0) - \Phi_{ij}(0) \Phi_{mn}(-\vec{\nu}) \frac{S(-\vec{\nu})}{d} \right)$$

$$+ \left(\frac{N}{\pi a} \right) \left(\frac{D}{d} \right) \Phi_{ij}(0) \Phi_{mn}(0) , \quad (28)$$

where

$$D = \left(\sum_{\vec{\nu}} {}' \nu^{-2} - \int \frac{d\vec{q}}{q^2} \right) + \sum_{\vec{\nu}} {}' \nu^{-2} \sum_{m=2}^{d} e^{2\pi i \vec{\nu} \cdot \vec{s}_m}$$

$$= -8.913633 \cdots + \sum_{\vec{\nu}} {}' \nu^{-2} [S(\vec{\nu}) - 1] . \quad (29)$$

The quantity D may be thought of as a lattice-structure constant, as it depends only upon the crystal structure and not upon the details of the electron distribution. The number $-8.913633 \cdots$ is the limit of the difference of the individually divergent sum and integral enclosed in parentheses in the preceding line. Details of the evaluation of D for various lattices are given in Appendix B of I. The D values for the lattices used in this paper are included in Table I.

For the reduction of the exchange matrix elements, we proceed analogously. Now the complex exponentials in $\vec{k}$ and $\vec{k}'$ do not cancel, and the $\vec{\nu}=0$ point leads to no singularities. The matrix element has the value

$$\langle \vec{k}_i \vec{k}_m' | r_{12}^{-1} | \vec{k}_n' \vec{k}_j \rangle = \frac{N}{\pi a} \sum_{\vec{\nu}} \frac{1}{|\vec{\nu} + \vec{k} - \vec{k}'|^2} \Phi_{in}(\vec{\nu}) \Phi_{jm}(-\vec{\nu}) . \quad (30)$$

In order to analyze the nature of the exchange energy, we write Eq. (30) in the form

$$\langle \vec{k}_i \vec{k}_m' | r_{12}^{-1} | \vec{k}_n' \vec{k}_j \rangle = \frac{N}{\pi a} \frac{1}{|\vec{k} - \vec{k}'|^2} \Phi_{in}(0) \Phi_{jm}(0)$$

$$+ \frac{N}{\pi a} \sum_{\vec{\nu}} {}' \nu^{-2} \Phi_{in}(\vec{\nu}) \Phi_{jm}(-\vec{\nu})$$

$$+ \frac{N}{\pi a} \sum_{\vec{\nu}} {}' \left(\frac{1}{|\vec{\nu} + \vec{k} - \vec{k}'|^2} - \frac{1}{\nu^2} \right) \Phi_{in}(\vec{\nu}) \Phi_{jm}(-\vec{\nu}) . \quad (31)$$

Equation (31) shows that the exchange energy consists of a free-electron-like contribution arising

from overlap charges, a Coulomb-like contribution arising from the nonuniformity of the charges, and a "correction" term. For the basis orbitals we found to be optimum, the free-electron part is significantly larger than the Coulomb and "correction" part. Since $|\vec{v}+\vec{k}-\vec{k}'|^{-2}$ approaches ν^{-2} rapidly as ν increases, we have a useful check for determining the computational precision of the exchange contribution to the Fock matrix.[5]

IV. WORKING FORMULAS

We are now in a position to use symmetry to simplify our expressions and write our working formulas in a more compact form. If we define

$$\phi_{ij}(\vec{q}) = \sum_{\vec{\mu}} \sum_{m=1}^{d} \langle \phi_i(\vec{r}) | e^{2\pi i a^{-1}\vec{q}\cdot\vec{r}} | \phi_j(\vec{r} - a\vec{\mu} - a\vec{s}_m) \rangle , \quad (32)$$

then we can write

$$\Phi_{ij}(\vec{q})$$

$$= \sum_{\vec{\mu}} \sum_{m,m'=1}^{d} \langle \phi_i(\vec{r} - a\vec{s}_m) | e^{2\pi i a^{-1}\vec{q}\cdot\vec{r}} | \phi_j(\vec{r} - a\vec{\mu} - a\vec{s}_{m'}) \rangle$$

$$= \left(\sum_{m=1}^{d} e^{2\pi i \vec{q}\cdot\vec{s}_m} \right)$$

$$\times \sum_{\vec{\mu}} \sum_{m'=1}^{d} \langle \phi_i(\vec{r}) | e^{2\pi i a^{-1}\vec{q}\cdot\vec{r}} | \phi_j(\vec{r} - a\vec{\mu} - a\vec{s}_{m'}) \rangle ,$$

or

$$\Phi_{ij}(\vec{q}) = S(\vec{q})\phi_{ij}(\vec{q}) . \quad (33)$$

Now that we have established that $\Phi_{ij}(\vec{q})$ is only needed for reciprocal-lattice vectors $\vec{q} = \vec{v}$, we may verify that $S(\vec{v})$ is either 0 or d. For the sc case, $S(\vec{v}) = 1$ for all $\vec{v}$. Since $S(0) = d$ for all symmetries,

$$S_{ij} = d^{-1}\Phi_{ij}(0) = \phi_{ij}(0) . \quad (34)$$

Similarly, T_{ij} of Eq. (18) reduces to

$$T_{ij} = \sum_{\vec{\mu}} \sum_{m=1}^{d} \langle \phi_i(\vec{r}) | -\tfrac{1}{2}\nabla^2 | \phi_j(\vec{r} - a\vec{\mu} - a\vec{s}_m) \rangle . \quad (35)$$

Furthermore, we note that the $\phi_{ij}(\vec{v})$ are the same for the set of all vectors $\vec{v}$ that are interrelated through the operations of the point group of the lattice. This set of equivalent vectors is called a star of vectors, and the number of these vectors within star t ($t = 1, 2, \ldots$) is denoted by g_t. Letting $\vec{v}_t$ be a representative vector from star t, we order the stars according to ascending values of ν_t. In cubic crystals, g_t can have values 1 [for $\vec{v}_t = (0, 0, 0)$], 6, 8, 12, 24, or 48, the last value occurring when $\vec{v}_t$ has an asymmetric relation to the symmetry directions.

Now, using Eq. (33) and the notion of stars of vectors, we can write for Eqs. (28) and (30)

$$\langle \vec{k}_l \vec{k}_m' | h | \vec{k}_j \vec{k}_n' \rangle = \frac{Nd}{\pi a} \sum_{t\neq 1} g_t \frac{S(\vec{v}_t)}{\nu_t^2} [\phi_{ij}(\vec{v}_t)\phi_{mn}(-\vec{v}_t)$$

$$- \phi_{ij}(\vec{v}_t)\phi_{mn}(0) - \phi_{ij}(0)\phi_{mn}(-\vec{v}_t)]$$

$$+ \left(\frac{Nd}{\pi a} \right) D\phi_{ij}(0)\phi_{mn}(0) , \quad (36)$$

$$\langle \vec{k}_l \vec{k}_m' | r_{12}^{-1} | \vec{k}_n' \vec{k}_j \rangle = \frac{Nd}{\pi a} \sum_{\vec{v}} \frac{S(\vec{v})}{|\vec{v}+\vec{k}-\vec{k}'|^2} \phi_{in}(\vec{v})\phi_{mj}(-\vec{v}) . \quad (37)$$

Finally, we summarize the working formulas for the computational process:

$$F_{ij}(\vec{k}) = T_{ij} + \frac{2\pi^2 k^2}{a^2} S_{ij} + V_{ij}$$

$$+ \frac{1}{\pi a} \sum_{t\neq 1} g_t \frac{S(\vec{v}_t)}{\nu_t^2} \sum_{mn} P_{mn}\phi_{ij}(\vec{v}_t)\phi_{mn}(-\vec{v}_t)$$

$$- \frac{1}{2\pi a} \sum_{t} g_t S(\vec{v}_t) \sum_{mn} Q_{mn}^t(\vec{k})\phi_{in}(\vec{v}_t)\phi_{mj}(-\vec{v}_t) , \quad (38)$$

$$V_{ij} = -\frac{1}{\pi a} \sum_{t\neq 1} g_t \frac{S(\vec{v}_t)}{\nu_t^2} \phi_{ij}(\vec{v}_t) , \quad (39)$$

$$P_{mn} = (2/d) \int c_m^*(\vec{k}')c_n(\vec{k}') d\vec{k}' \quad (40)$$

$$Q_{mn}^t(\vec{k}) = \left\langle \frac{2}{d} \int \frac{c_m^*(\vec{k}')c_n(\vec{k}') d\vec{k}'}{|\vec{v}+\vec{k}-\vec{k}'|^2} \right\rangle_t , \quad (41)$$

where $\langle \cdots \rangle_t$ indicates that $\vec{v}$ is to be averaged over members of star t.

Equation (7) becomes

$$\sum_{mn} c_m^*(\vec{k})\phi_{mn}(0)c_n(\vec{k}) = 1 , \quad (42)$$

and ϕ_{ij}, S_{ij}, and T_{ij} are given by Eqs. (32), (34), and (35). By comparison of Eq. (10) with Eq. (38), one observes that terms proportional to S_{ij} and independent of $\vec{k}$ have been dropped. These can be accounted for by an additive change in $\epsilon(\vec{k})$. An energy expression consistent with Eq. (38) is

$$E = N \left[\int d\vec{k} \sum_{ij} c_i^*(\vec{k}) \left(F_{ij}(\vec{k}) + T_{ij} \right. \right.$$

$$\left. \left. + \frac{2\pi^2 k^2}{a^2} S_{ij} + V_{ij} \right) c_j(\vec{k}) + \frac{Dd}{2\pi a} \right] . \quad (43)$$

If the Hartree-Fock equations are satisfied, we can also write

$$E = N \left[\int d\vec{k}\, \epsilon(\vec{k}) + \sum_{ij} \int d\vec{k}\, c_i^*(\vec{k}) \right.$$

$$\left. \times \left(T_{ij} + \frac{2\pi^2 k^2}{a^2} S_{ij} + V_{ij} \right) c_j(\vec{k}) + \frac{Dd}{2\pi a} \right] . \quad (44)$$

V. NUMERICAL TECHNIQUES

Our formulation of the Hartree-Fock method for atomic hydrogen crystals presents three major computational problems. These are (i) the calculation of the Fourier-transform quantities $\phi_{ij}(\vec{q})$ from Eq. (32) and T_{ij} from Eq. (35); (ii) identification of suitable forms for $c_i(\vec{k})$, $\epsilon(\vec{k})$, and the shape of the Fermi surface as functions of $\vec{k}$, such that the $\vec{k}$

and $\vec{k}'$ integrations are manageable and the iterations needed to solve the Hartree–Fock equations can be executed efficiently; (iii) the calculation of $Q_{mn}^t(\vec{k})$ from Eq. (41).

Let us first consider the $\phi_{ij}(\vec{q})$. We could proceed by calculating term by term in Eq. (32). In fact, for $1s$ Slater-type orbitals (STO's) we developed a numerically stable method for the evaluation of these Fourier transforms of two-center STO products.[9] However, we can take full advantage of the lattice sum through the use of the Fourier-convolution theorem. We write, therefore,

$$\phi_{ij}(\vec{q}) = \sum_{\vec{\mu}} \sum_{m=1}^{d} \left[\phi_i^*(\vec{r}) \phi_j(\vec{r} - a\vec{\mu} - a\vec{s}_m) \right]^T(\vec{q})$$

$$= a^{-3} \sum_{\vec{\mu}} \int d\vec{p} \, \phi_i^{*T}(\vec{p}) \phi_j^T(\vec{q} - \vec{p}) S(\vec{q} - \vec{p}) e^{2\pi i (\vec{q} - \vec{p}) \cdot \vec{\mu}} \, .$$

Again invoking Eq. (20), and noting that $S(-\vec{\nu}) = S(\vec{\nu})$, we obtain

$$\phi_{ij}(\vec{q}) = a^{-3} \sum_{\vec{\nu}} S(\vec{\nu}) \phi_i^{*T}(\vec{q} + \vec{\nu}) \phi_j^T(-\vec{\nu}) \, . \tag{45}$$

Similarly, we derive

$$T_{ij} = \sum_{\vec{\mu}} \sum_{m=1}^{d} \langle \phi_i(\vec{r}) | -\tfrac{1}{2} \nabla^2 | \phi_j(\vec{r} - a\vec{\mu} - a\vec{s}_m) \rangle$$

$$= a^{-3} \sum_{\vec{\nu}} S(\vec{\nu}) \phi_i^{*T}(\vec{\nu}) [-\tfrac{1}{2} \nabla^2 \phi_j(\vec{r})]^T(-\vec{\nu})$$

or

$$T_{ij} = \frac{2\pi^2}{a^5} \sum_t g_t \nu_t^2 S(\vec{\nu}_t) \phi_i^{*T}(\vec{\nu}_t) \phi_j^T(-\vec{\nu}_t) \, . \tag{46}$$

We refer to Appendix A for explicit formulas for ϕ_{ij} and T_{ij} when specific choices for the ϕ_i are made. Note that Eqs. (45) and (46) now involve only the knowledge of the Fourier transforms of individual ϕ_i. We thus have the remarkable result that all crystal integrals are expressed in sums that require one-center Fourier-transform integrals only. We found these sums to converge very satisfactorily for typical choices of ϕ_i.[5]

Next we discuss the analytical representations of $c_i(\vec{k})$ and $\epsilon(\vec{k})$, and the description of the Fermi surface. We note that the restricted Hartree–Fock scheme we adopted necessitates that $c_i(\vec{k})$ be totally symmetric under the cubic-point-group operations. Evidently the $\epsilon(\vec{k})$ and the shape of the Fermi surface should have this symmetry as well. Therefore we found it convenient to introduce expansions in k^2 and normalized cubic harmonics $T_u(u = 1, 2, \ldots)$ of the totally symmetric representation of the cubic point group[5]:

$$c_i(\vec{k}) = \sum_u \sum_{p \geq l_u} c_{pu}^i k^{2p} T_u(\Omega) \, , \tag{47}$$

$$\epsilon(\vec{k}) = \sum_u \sum_{p \geq l_u} \epsilon_{pu} k^{2p} T_u(\Omega) \, , \tag{48}$$

$$\bar{k}(\Omega) = \sum_u f_u T_u(\Omega) \, . \tag{49}$$

Here k and Ω are the radial and angular coordinates of $\vec{k}$, and $\bar{k}(\Omega)$ is the radial coordinate of the Fermi surface in the direction Ω. The angular-momentum quantum number of T_u is l_u, and the T_u are ordered according to ascending values of l_u. The cubic harmonic T_u is constructed from completely symmetric homogeneous polynomials, all of (even) degree l_u in the coordinates x, y, and z. For details of the construction we use for the T_u, we refer to Appendix I of Ref. 5.

In $\vec{k}$ integrations the c_m occur as products $c_m^* c_n$. When multiplied together and using the cubic-harmonic equivalent of the Clebsch–Gordan expansion, we get

$$c_m^*(\vec{k}) c_n(\vec{k}) = \sum_{uu'v} \sum_{p \geq l_u} \sum_{p' \geq l_{u'}} c_{pu}^{m*} c_{p'u'}^n D_{uu'v} k^{2p+2p'} T_v(\Omega) \, , \tag{50}$$

where $D_{uu'v}$ is the cubic Clebsch–Gordan coefficient given by

$$T_u(\Omega) T_{u'}(\Omega) = \sum_v D_{uu'v} T_v(\Omega) \, . \tag{51}$$

In Eq. (50), l_u and $l_{u'}$ are the angular-momentum quantum numbers of T_u and $T_{u'}$, respectively. In actual calculations we condense Eq. (50) into

$$c_m^*(\vec{k}) c_n(\vec{k}) = \sum_u \sum_{p \geq l_u} c_{pu}^{mn} k^{2p} T_u(\Omega) \, . \tag{52}$$

The quantity P_{mn} [Eq. (40)] requires the evaluation of integrals like

$$\int d\vec{k} \, k^{2p} T_u(\Omega) = \int d\Omega \int_0^{\bar{k}(\Omega)} dk \, k^{2p+2} T_u(\Omega)$$

$$= \frac{1}{2p+3} \int d\Omega \, [\bar{k}(\Omega)]^{2p+3} \, . \tag{53}$$

Repeatedly using Eq. (51) and noting that only the integration over $T_1 = (4\pi)^{-1/2}$ survives, we obtain

$$\int d\vec{k} \, k^{2p} T_u(\Omega) = \frac{(4\pi)^{1/2}}{2p+3} (\underline{E}^{2p+3})_{u1} \, , \tag{54}$$

where $\underline{E}$ is a matrix with elements

$$E_{uu'} = \sum_v f_v D_{vuu'} \, . \tag{55}$$

We can now write for P_{mn}

$$P_{mn} = \left(\frac{2}{d}\right) \sum_u \sum_{p \geq l_u} \frac{(4\pi)^{1/2}}{2p+3} c_{pu}^{mn} (\underline{E}^{2p+3})_{u1} \, . \tag{56}$$

Finally, the evaluation of the quantity $Q_{mn}^t(\vec{k})$ presents the additional difficulty of the factor $|\vec{\nu} + \vec{k} - \vec{k}'|^{-2}$ and the averaging over the star t. If $\nu_t > k + k'$, it is natural to use an expansion involving k/ν and k'/ν, and $T_u(\Omega_k)$ and $T_{u'}(\Omega_{k'})$. The expansion is[5]

$$\frac{1}{|\vec{v}+\vec{k}-\vec{k}'|^2} = \frac{16\pi^2}{\nu^2} \sum_{uu'v} \sum_{s,s'=0} G_{vuu'}^{ss'} \left(\frac{k}{\nu}\right)^{l+2s} \left(\frac{k'}{\nu}\right)^{l'+2s'} T_v(\Omega_v)T_u(\Omega_k)T_{u'}(\Omega_{k'}) + \text{less-symmetric terms}, \qquad (57)$$

where

$$G_{vuu'}^{ss'} = (-)^l D_{vuu'} \frac{(2s+2s'+l+l'-L-1)!!(2s+2s'+l+l'+L)!!}{(2s+2l+1)!!(2s)!!(2s'+2l'+1)!!(2s')!!} , \qquad (58)$$

and l, l', L are angular quantum numbers of T_u, $T_{u'}$, and T_v, respectively. The less-symmetric terms in Eq. (57) vanish on integration over $\vec{k}'$ and the averaging $\langle \cdots \rangle_t$ in $Q_{mn}^t(\vec{k})$. Except for $\vec{v} = (0, 0, 0)$ and $(1, 0, 0)$ in the sc case, and $\vec{v} = (0, 0, 0)$ in the bcc and fcc cases, Eq. (57) can be used for all star vectors $\vec{v}_t$. Since this formula is symmetric in the orientations of $\vec{v}_t$, the directional averaging in $Q_{mn}^t(\vec{k})$ can be dropped. After applying Eq. (54), we obtain the following expression for $\nu_t > 1$:

$$Q_{mn}^t(\vec{k}) = \left(\frac{2}{d}\right)\left(\frac{16\pi^2}{\nu_t^2}\right) \sum_w \sum_{p \geq l_w} \sum_{ss'} \sum_{vuu'}$$

$$\times \frac{c_{pw}^{mn} G_{vuu'}^{ss'} T_v(\Omega_v) k^{l+2s} T_u(\Omega_k)}{(2p+2s'+l'+3)\nu_t^{l+l'+2s+2s'}} \left(\underline{E}^{2p+2s'+l'+3}\right)_{wu'} . \qquad (59)$$

Here Ω_v denotes the angular coordinates of $\vec{v}_t$. This expression looks terrifying because of the infinite summations and the (p, w) summations for the proper representation of $c_m^* c_n$. In practice, however, only a small number of terms need to be retained to give the exchange energy to four significant figures. In addition, for large ν_t we are helped by the convergence of the quantities multiplying the $Q_{mn}^t(\vec{k})$ in the expression for the Fock matrix. We refer to Ref. 5 for a detailed numerical analysis of Eq. (59).

For the small star vectors $\vec{v}_t$ we had to resort to an entirely different expansion[10]:

$$|\vec{v}+\vec{k}-\vec{k}'|^{-2} = \frac{2\pi}{k'|\vec{v}+\vec{k}|} \sum_w T_w(\Omega')T_w(\Omega_{k'})Q_L\left(\frac{1+\omega^2}{2\omega}\right)$$

$$+ \text{less-symmetric terms}, \qquad (60)$$

where Q_L is a Legendre function of the second kind, Ω' is the direction of $\vec{v}+\vec{k}$, L is the angular-momentum quantum number of T_w, and $\omega = k'/|\vec{v}+\vec{k}|$. We define

$$I_{pL}(\bar{\omega}) = \int_0^{\bar{\omega}} \omega^{p+1} Q_L\left(\frac{1+\omega^2}{2\omega}\right) d\omega , \qquad (61)$$

with $\bar{\omega} = \bar{k}(\Omega_{k'})/|\vec{v}+\vec{k}|$. Combining now Eqs. (41), (52), (60), and (61), we find

$$Q_{mn}^t(\vec{k}) = \left(\frac{2}{d}\right)\Big\langle \sum_u \sum_{p \geq l_u} c_{pu}^{mn} \frac{2\pi}{|\vec{v}+\vec{k}|^{-2p-1}} \sum_{u'v} T_v(\Omega')$$

$$\times D_{vuu'} \int T_{u'}(\Omega_{k'}) I_{2p,L}(\bar{\omega}) d\Omega_{k'} \Big\rangle_t , \qquad (62)$$

where l and L are the angular-momentum quantum numbers of T_u and T_v, respectively. As in Eq.

(57), the less-symmetric terms do not survive the integration over $\vec{k}'$ and the $\vec{v}$ orientation averaging. The integration in Eq. (61) is done analytically, whereas the angular integration in Eq. (62) is performed numerically. The $\vec{v}$ directional averaging is done directly. For mathematical and numerical details in the calculation of the I_{pL} and the numerical integration over Ω_k, we refer to Appendix B. Expression (62) is completely general. However, the numerical integration and the necessity of direct averaging over $\vec{v}$ directions make this method considerably slower than that described for large ν. We therefore use it only when necessary.

VI. ORGANIZATION OF COMPUTER PROGRAM

It is appropriate at this point to summarize the successive operations involved in a typical complete Hartree–Fock calculation. In practice we used different programs for different lattice structures. The programs involved the following steps:

Step 1. Reading and printing of input data. These data are the lattice spacing a, specification of basis orbitals ϕ_i, number of stars in $\vec{v}_t$ sums, and number of radial and angular expansion terms for $c_i(\vec{k})$, $\epsilon(\vec{k})$, and $\bar{k}(\Omega)$ [Eqs. (47)–(49)] and for $Q_{mn}^t(\vec{k})$ from Eq. (59). Additional input data are necessary for iteration control and least-squares-fitting procedures to be discussed below.

Step 2. Calculations of quantities preparatory to Hartree–Fock iterations. These quantities are the list of star vectors, the $\phi_{ij}(\vec{v}_t)$, T_{ij}, V_{ij}, cubic harmonics $T_u(\Omega)$ and related quantities, expansion coefficients for $Q_{mn}^t(\vec{k})$ according to Eq. (59), and initialization of $c_i(\vec{k})$ and the shape of the Fermi surface. We usually started with full occupancy of one of the basis Bloch orbitals, and a spherical Fermi surface. Finally, the $\vec{k}$ vectors are specified for which the Hartree–Fock equations are to be solved. The radial values k are placed at equal intervals in k^2 from 0 to k_F^2, where k_F is the Fermi sphere radius in units $(2\pi/a)$. The $\vec{k}$ orientations are taken to be those of independent star directions.

Step 3. Construction of $F_{ij}(\vec{k})$ matrix for a set of $\vec{k}$ vectors. The reciprocal-lattice summations in Eq. (38) are extended so as to ensure accuracy to four significant figures. In the current problem, this involves about 143 stars of $\vec{v}_t$ vectors ($\nu_t \leq 10$). We usually considered twelve radial k values and ten directions, totaling 120 $\vec{k}$ vectors.

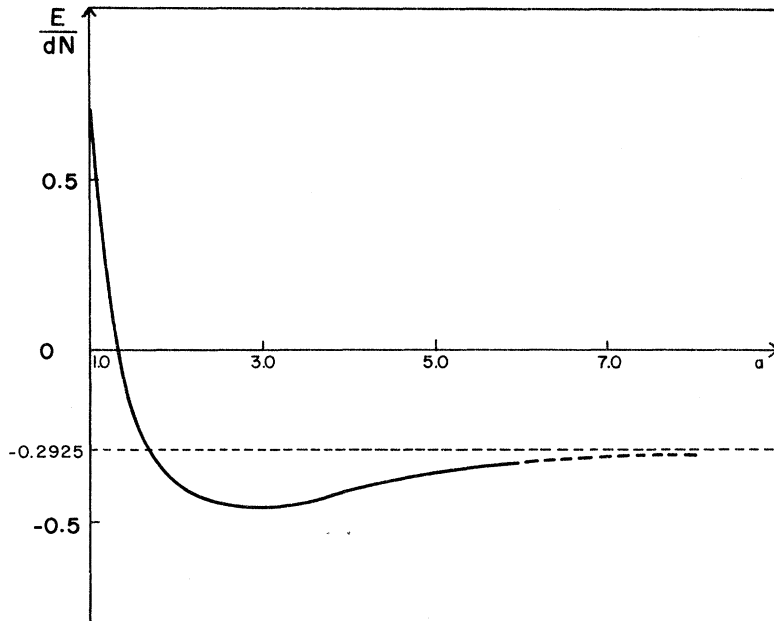*Step* 4. Solution for eigenvalue $\epsilon(\vec{k})$, coefficients

FIG. 1. Total energies per atom E/Nd (in hartrees) vs lattice spacing a (in bohrs) for a sc atomic-hydrogen crystal. The Bloch orbital is built from one $1s$ STO with screening parameter $\zeta = 1.2$. The dashed part of the curve is not calculated but graphically extrapolated.

$c_i(\vec{k})$ for each $\vec{k}$ vector [Eq. (9)].

Step 5. Conversion of $\epsilon(\vec{k})$ and $c_i(\vec{k})$ to analytical expressions by a least-squares-fitting process [Eqs. (47) and (48)]. This involves a fitting to functions $k^{2p}T_u(\Omega)$. In order to achieve an accuracy of four significant figures, we found it to be necessary to perform this step in double precision.

Step 6. Calculation of new Fermi surface [Eq. (49)]. From the $\epsilon(\vec{k})$ expansion, the requirement of constant energy at the Fermi surface and reciprocal-space volume $\frac{1}{2}d$ in units $(2\pi/a)^3$, a simple nonlinear problem for the coefficients f_u follows. Because the Fermi surface has only a slight distortion from a spherical shape, the coefficients f_u may be obtained by a rapidly convergent iterative procedure.

Step 7. Check whether Hartree–Fock convergence criterion has been met. If the relative difference between current and previous values for $\int \epsilon(\vec{k})d\vec{k}$ is less than 5×10^{-4}, we stop the iterations. If not, another cycle beginning at Step 3 is performed.

Step 8. Calculation of total energy and printing of final results when calculation has converged. With Eq. (44) and the analytical forms of $c_i(\vec{k})$ and $\epsilon(\vec{k})$, E/Nd is computed, and it and the expansion coefficients in Eqs. (47) to (49) are printed.

We excuted the calculations on Univac 1108 equipment. With our current programs, typical calculations take 3, 2, and 1 min. for sc, bcc, and fcc structures, respectively, when two ϕ_i per lattice site are used.

VII. RESULTS

All results to be described here were obtained by numerical methods yielding at least four signif-

icant figures in the band energies $\epsilon(\vec{k})$.

Our first calculations involved the use of one $1s$ STO basis orbital ϕ_i per lattice site. Numerical details involving these ϕ_i are given in Appendix A. In Fig. 1 we present a typical plot of E/Nd values as a function of lattice spacing a. The curve shows the familiar flaw of the restricted Hartree–Fock method in that the forced double occupancy of the Bloch functions introduces unphysical electron-repulsion terms in the total energy at large lattice spacings. In fact, when only one ϕ_i per lattice site is used, the double occupancy leads to an easily calculable energy in the limit of infinite lattice spacing:

$$\lim_{a \to \infty} (E/Nd) = \langle \phi_1 | -\tfrac{1}{2}\nabla^2 - 1/r | \phi_1 \rangle + \tfrac{1}{4}\langle \phi_1\phi_1 | r_{12}^{-1} | \phi_1\phi_1 \rangle .$$

(63)

For $1s$ STO's with screening parameter ζ, Eq. (63) can be evaluated to yield

$$\lim_{a \to \infty} (E/Nd) = (\tfrac{1}{2}\zeta^2 - \zeta) + \tfrac{1}{4}(\tfrac{5}{8}\zeta) .$$

(64)

The curve in Fig. 1 has been graphically extrapolated to this limit from approximately $a = 6$ bohr, where our numerical methods begin to exhibit inadequacy. Additional detail regarding results at this approximation level may be found in our earlier work.[7]

We sought to minimize the energy under variations of the screening parameter and lattice spacing with one $1s$ STO per lattice site. The best results are summarized in Table II. Table III typifies the $\epsilon(\vec{k})$ values obtained as a function of $\vec{k}$ for fcc crystals. Harris and Monkhorst[7] give similar data for the sc case. Both sets of data have in common the

TABLE II. Total energies per atom E/Nd (in hartrees) for atomic-hydrogen crystals of nearest-neighbor distances δ (in bohrs), based on one $1s$ orbital per lattice site with screening parameter ζ. The entries with $\zeta = 0$ correspond to the use of plane-wave orbitals.

	sc			bcc			fcc	
δ	ζ	E/Nd	δ	ζ	E/Nd	δ	ζ	E/Nd
2.68	1.20	−0.4610	2.90	1.25	−0.4653	2.90	1.25	−0.4641
2.68	1.30	−0.4629	2.90	1.28	−0.4655	2.90	1.30	−0.4647
2.68	1.35	−0.4610	2.90	1.30	−0.4653	2.90	1.35	−0.4636
2.78	1.20	−0.4621	3.00	1.20	−0.4638	3.00	1.20	−0.4639
2.78	1.25	−0.4631	3.00	1.25	−0.4655	3.00	1.25	−0.4653
2.78	1.30	−0.4622	3.00	1.30	−0.4640	3.00	1.30	−0.4650
2.88	1.20	−0.4620	3.10	1.18	−0.4639	3.10	1.20	−0.4645
2.88	1.25	−0.4621	3.10	1.23	−0.4646	3.10	1.25	−0.4651
2.88	1.30	−0.4599	3.10	1.28	−0.4634	3.10	1.30	−0.4639
∞	1.20	−0.2925	∞	1.35	−0.2278	∞	1.30	−0.2519
2.56	0.00	−0.4045	2.77	0.00	−0.4143	2.85	0.00	−0.4143
2.66	0.00	−0.4052	2.87	0.00	−0.4149	2.95	0.00	−0.4148
2.76	0.00	−0.4048	2.97	0.00	−0.4144	3.05	0.00	−0.4144

very small $\vec{k}$-orientation dependence of $\epsilon(\vec{k})$. This invariably leads to nearly spherical Fermi surfaces, the largest distortions coming in the [100] direction for the sc lattice.

In the next series of calculations, two $1s$ STO's were taken per lattice site, starting from the best single-ζ results. We did not observe any significant lowering of E/Nd values, nor did we find noticeable changes in the Bloch functions. We suspected a near-linear–dependence problem between the basis Bloch orbitals. This was suggested by the near equality of $S_{11}S_{12}$ and S_{12}^2 values, where S_{ij} are the overlap integrals from Eq. (34). The overlapping of the $1s$ STO's possibly washes out the differences between the basis Bloch orbitals. A similar problem sometimes arises in tight-binding–type calculations.[11]

We tried to circumvent the possible linear-dependence problem by introducing so-called "cutoff" basis orbitals. These orbitals have $1s$ STO behavior inside the Wigner–Seitz (WS) cells centered at each lattice site, and are zero outside. For numerical details we refer to Appendix A. We found for the sc structure that two of these orbitals lead to Hartree–Fock results that are virtually indistinguishable from the results obtained with the conventional STO's. Relevant data can be found in Harris and Monkhorst.[7] Addition of a third "cutoff" orbital again left the results essentially unchanged.

This finding led us to presume that the Bloch orbitals $|\vec{k}\rangle$ based on the conventional STO's and the cutoff orbitals are very similar, and indeed, we found this to be the case. The two Bloch functions for a sc lattice have been plotted in Fig. 2. In view of this and the results above, we did not pursue the use of cutoff orbitals for bcc and fcc

structures.

Finally, we wanted to investigate whether our results had approached the Hartree–Fock limit. The essential equivalence of the results obtained above with the two types of ϕ_i already strongly suggests that we are very close to that limit. The inclusion of higher ns STO's in the basis does not affect the results. These would only influence the behavior of $|\vec{k}\rangle$ in the internuclear regions, but this can be accounted for by the $1s$ STO's. We analyzed the effect of a ϕ_i with angular dependence. The simplest such function compatible with the A_{1g} cubic symmetry is a $5g$ STO. We performed calculations using $1s$ and $5g$ STO's. For numerical details, see Appendix A. We concluded that no ζ value can be found at which the $5g$ orbital contributes significantly to $|\vec{k}\rangle$ or E/Nd. Numerically this is caused by the small $1s$-$5g$ off-diagonal Fock matrix element, combined with a large $5g$ diagonal element. The latter contains a large kinetic-energy contribution arising from the g angular symmetry.

Concluding, we can state that we essentially reached the Hartree–Fock limit for all cubic atomic-hydrogen crystals. The Fermi surfaces are practically spherical. The Hartree–Fock Bloch functions are well represented by a single basis Bloch orbital built from $1s$ STO's. The relevant data defining the wavefunctions, energies, and lattice spacing are given in Table I. (See *Note added in proof.*)

VIII. DISCUSSION

The optimum crystal structures predicted from our calculations for the atomic-hydrogen crystal are in general agreement with previous studies. Wigner and Huntington,[12] and later Kronig, De Boer, and Korringa,[13] using the WS method, obtained a nearest-neighbor distance of 2.81 bohrs for the bcc structure, reasonably close to our value

TABLE III. Band energies $\epsilon(\vec{k})$ (in hartrees) and radial coordinates $\vec{k}(\Omega)$ [in units $(2\pi/a)$] of the Fermi surface in reciprocal-lattice directions $[uvw]$, for an fcc atomic-hydrogen crystal of linear unit-cell dimension a. The Bloch orbital is built from one $1s$ STO per lattice site with $\zeta = 1.30$ and nearest-neighbor distance $\delta = 2.99$ bohr. If spherical, the Fermi surface would have $\vec{k} = 0.781\,59$.

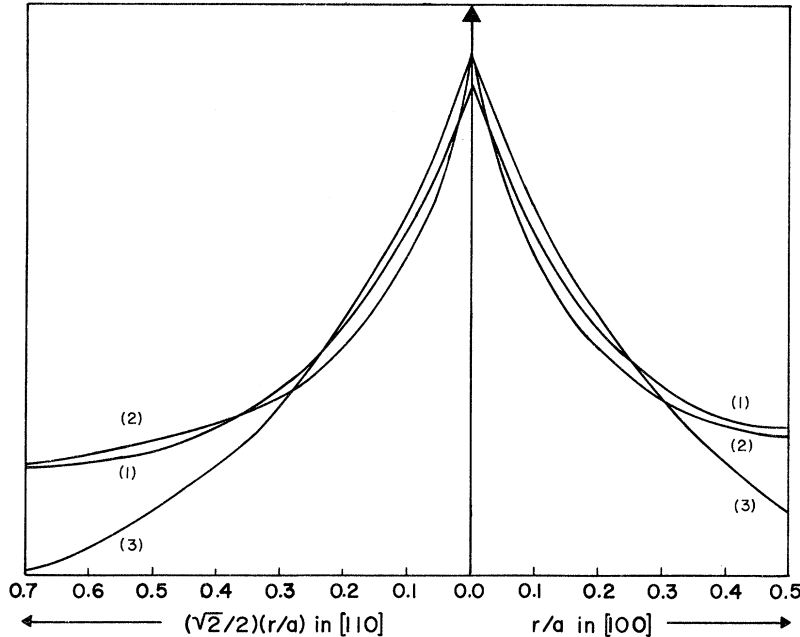| k	[100]	[110]	[111]	[210]	[211]
0.217	−0.7221	−0.7221	−0.7221	−0.7221	−0.7221
0.375	−0.5780	−0.5781	−0.5781	−0.5780	−0.5781
0.485	−0.4306	−0.4308	−0.4309	−0.4307	−0.4308
0.574	−0.2788	−0.2792	−0.2794	−0.2790	−0.2792
0.650	−0.1206	−0.1213	−0.1217	−0.1210	−0.1214
0.718	0.0483	0.0471	0.0464	0.0477	0.0469
0.782	0.2509	0.2474	0.2472	0.2509	0.2471
$\vec{k}(\Omega)$	0.7812	0.7817	0.7819	0.7815	0.7817

FIG. 2. Magnitude of crystal orbitals $|k\rangle$ (with $\vec{k}=0$) as a function of position (units of lattice spacing a) in the [100] and [110] directions of a sc hydrogen crystal with $a=2.75$ bohr. These orbitals are normalized over the WS cell. Also shown is the normalized free-hydrogen-atom $1s$ orbital. Curve 1: crystal orbital built from one conventional $1s$ STO with $\zeta=1.20$. Curve 2: crystal orbital built from three "cutoff" orbitals with $\zeta_1=0.17$; $\zeta_2=1.0$; $\zeta_3=3.0$. Curve 3: free-hydrogen-atom $1s$ orbital.

of about 2.9 bohr. Our energies are not directly comparable with theirs, since the latter contain estimates of the correlation energy which are not considered in Hartree–Fock calculations. The molecular-orbital (MO) calculations of Calais[14] can be compared with our work. We agree qualitatively with his results. Though the equilibrium nearest-neighbor distance for the sc structure is quite different from that for the bcc and fcc structures, their densities are nearly the same, namely, approximately 0.05 atoms/bohr^3.

For all three of the cubic structures we considered, the Hartree–Fock energies per atom were found to be above the free-atom value of -0.5 hartree. Even after our estimates of correlation energy are included we find no stability relative to the isolated atoms. If we tentatively make the reasonable assumption that the correlation energies are comparable in the three structures, we conclude that the bcc and fcc structures are stable relative to the sc structure. However, the energy difference between the bcc and fcc structures is so small that it would be imprudent to take seriously the indication that the bcc structure is the more stable. Taken alone, our data do not provide information as to the stability of the atomic (metallic) crystal relative to a molecular (insulating) solid. However, our work may presumably be used in connection with other studies to refine recent estimates relating to this stability problem.[15] We note that the situation for the hydrogen crystal is quite different from that found for lithium. Our preliminary studies on lithium crystals[16] already show that at the Hartree–Fock level an atomic crystal would be

stable relative both to Li_2 molecules and to isolated Li atoms. The significant difference between the hydrogen and lithium crystals may be due to the s-p near degeneracy in the lithium valence shell, permitting neighboring Li atoms to form bonding electronic structures which are not possible for H atoms.

Turning now to the wave functions, we note (cf. Fig. 2) that the Hartree–Fock crystal orbitals possess nearly the same degree of spatial inhomogeneity as do the free-atom wave functions. Since the crystal orbitals deviate significantly from plane waves, we regarded it as of interest to identify the energy contribution associated with the inhomogeneity. We therefore calculated the energies for each crystal structure using plane-wave orbitals. These energies may be obtained from our present formalism by setting $\zeta=0$, where ζ is the screening parameter associated with a STO. If we assume also a spherical Fermi surface, we have

$$E_{\zeta=0}=Nd\left(\frac{6\pi^2}{5a^2}k_F^2-\frac{3}{2a}k_F+\frac{D}{2\pi a}\right),\qquad(65)$$

with $k_F=(3d/8\pi)^{1/3}$. The first term arises from the kinetic energy, the second is the exchange term, and the last term describes the potential energy of the nuclei and the uniform distribution of the electrons. As before, a is the dimension of the compound unit cell containing d atoms.

Values of $E_{\zeta=0}$ are included in Table II. It may be seen that the accurate Hartree–Fock energies are 0.05–0.06 hartree, or about 15% below the energies based on plane-wave functions. This energy difference is large enough to suggest that accurate
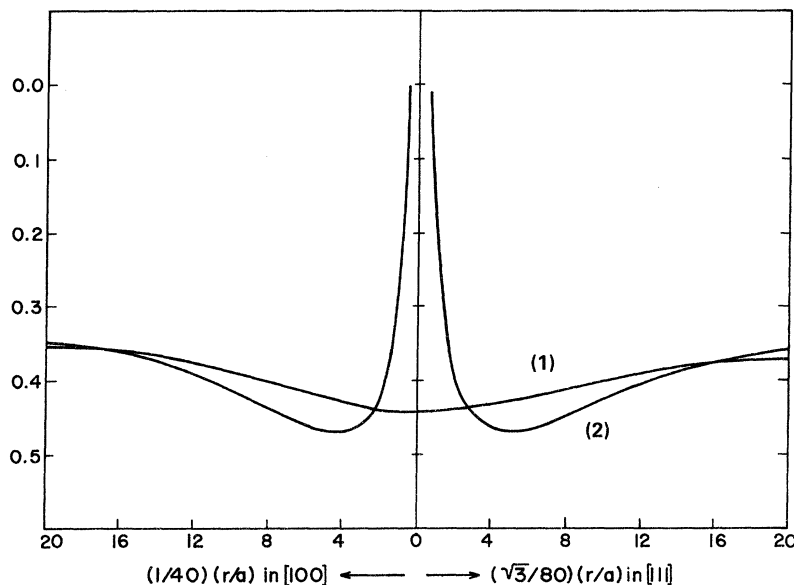
FIG. 3. Comparison of effective-exchange potentials (hartrees) calculated in different ways for a bcc atomic-hydrogen crystal of lattice spacing $a=3.3$ bohrs. Crystal orbitals built from one $1s$ STO with $\zeta=1.30$. Curve 1: direct evaluation of potential by Eq. (C8). Curve 2: evaluation by Eq. (C9), by method involving use of Hartree-Fock equations.

functions should be used not only to obtain the Hartree–Fock energy but also in correlation-energy calculations. To date correlation energies in inhomogeneous systems have generally been estimated perturbatively using plane-wave unperturbed states.[17]

The existence of accurate Hartree–Fock wave functions also provides an opportunity to assess the effect of spatial inhomogeneity upon the electron-exchange energy. One way to examine this question is to obtain the effective-exchange potentials necessary to reproduce the Hartree–Fock results and to compare these with approximate potentials predicted from studies of the homogeneous electron gas. Exchange potentials in so-called "statistical approximations" have been put forth by Slater,[18] Gaspar,[19] and Kohn and Sham.[20] These formulations involve use of the expression for the exchange energy of a homogeneous electron gas, replacing the (constant) electron density by the local density $\rho(\vec{r})$ of an inhomogeneous system. The Slater and Kohn–Sham potentials can be written in the common form

$$V_{X\alpha}(\vec{r}) = -(3\alpha/2\pi)[3\pi^2\rho(\vec{r})]^{1/3}, \qquad (66)$$

where $\alpha=1$ yields the Slater formula and $\alpha=\frac{2}{3}$ that of Kohn and Sham. This so-called $X\alpha$ potential is being used extensively in approximate atomic, molecular, and solid-state calculations.[21,22] According to a discussion by Hohenberg and Kohn,[23] a formula of this sort should be appropriate when the density is sufficiently slowly varying. The value $\alpha=\frac{2}{3}$ corresponds to the application of the variation theorem to the "statistical" total energy, while the value $\alpha=1$ is obtained by substitution of the approximation into the Hartree–Fock equations. We may note

that the inherently nonlocal nature of the exchange operator has been suppressed by the absence of any $\vec{k}$ dependence in the formula for $V_{X\alpha}(\vec{r})$.

We generated effective potentials from our Hartree–Fock calculations for comparison with Eq. (66) by methods described in some detail in Appendix C. For ease in interpretation we averaged over the direction of $\vec{k}$ so as to obtain real potentials. We derived two alternative expressions for the exchange potential which would be identical if the Hartree–Fock equations were exactly satisfied for all $\vec{r}$. The expression resulting from direct evaluation of the exchange energy, Eq. (C8), is that which should be used for comparison with other work. The expression using the Hartree–Fock equations, Eq. (C9), is of interest because its comparison with the other expression gives an indication of the exactness with which the Hartree–Fock equations are satisfied. As shown in Fig. 3, these two expressions give exchange potentials which are in close agreement over most of the WS cell, but which diverge strongly from each other close to the nuclei. The discrepancy arises because the cusp conditions are not exactly met at the nuclei, and corresponds to energy errors below the four-significant-figure level claimed in our calculations. The comparison indicates that Eq. (C8) generates an exchange potential which may reliably be used in further discussion.

Figure 4 gives the results of a comparison of the accurate direction-averaged exchange potentials with the Kohn–Sham and Slater approximations. We see that at $k=k_F$ the accurate potential agrees well with the Kohn–Sham result in the region of greatest density homogeneity, but differs systematically in the highly inhomogeneous region near
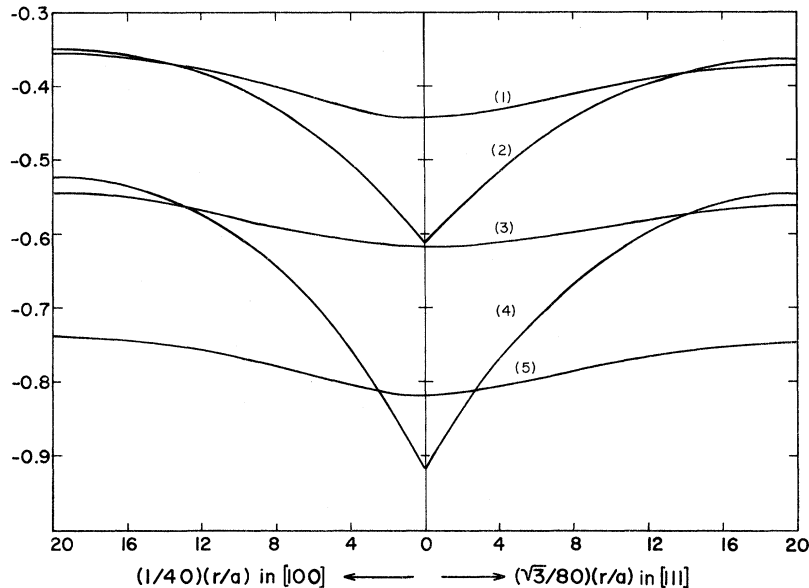
FIG. 4. Comparison of approximate effective-exchange potentials with those obtained in this study for a bcc atomic-hydrogen crystal of lattice spacing $a = 3.3$ bohrs. Crystal orbitals built from one $1s$ STO with $\zeta = 1.30$. Curve 1: this work, for $k = k_F$; curve 2: Kohn–Sham approximate potential; curve 3: this work, potential averaged over occupied $\vec{k}$ values; curve 4: Slater approximate potential; curve 5: this work, $k = 0$.

the nuclei. The region of significant disagreement is only a few percent of the volume of the WS cell. The exact potential moves to lower energy as k decreases, at $k = 0$ falling well below the Slater approximation. The average of the exchange potential over the occupied $\vec{k}$ values is also plotted, and it is seen to approach the Slater approximation in the more homogeneous region.

The drastic difference between the Kohn–Sham and the accurate-exchange potentials at $k \neq k_F$ does not necessarily indicate a failure of the Kohn–Sham approximation, as the eigenvalue in the Kohn–Sham self-consistent equations does not have the same significance as in the exact calculations. To the extent that the accurate and Kohn–Sham curves differ by a constant energy, they will predict the same self-consistent wave functions. It may be seen from Fig. 4 that the accurate-exchange potential differs with k much more nearly by the addition of a k-dependent constant than by a k-dependent scale factor or a more complicated k dependence. We therefore conclude that the Kohn–Sham approximation may be viable for obtaining wave functions, even for k values far from k_F. A k-dependent approximate potential has been suggested by Liberman.[24] That potential differs qualitatively from the exact potential in its behavior at the nuclei. It therefore appears that of the simple approximate exchange potentials, the Kohn–Sham formula will most closely reproduce the Hartree–Fock wave function.

Finally, we return to the question of our choice of $\vec{k}$ dependence for the basis Bloch orbitals. The fact that we nearly reach the Hartree–Fock limit with only one basis orbital is an indication that its $\vec{k}$ dependence is nearly optimal. We note that our

choice can be interpreted as a lattice-modulated plane wave, and that this wave function is intermediate in character between the conventional tight-binding and the orthogonalized-plane-wave functions.[16]

Note added in proof. It should be pointed out that our results are near-HF in a symmetry-restricted sense. So far we have only considered basis orbitals with A_{1g} symmetry, thus leading to a lattice-periodic factor in the Bloch orbitals with this symmetry only. Though some lower-symmetric components enter the Bloch orbitals through the plane-wave factor we clearly have not exhausted the full HF-variational freedom. Preliminary investigations have indicated that this has a small energetic effect in the hydrogen crystals. The HF Bloch orbitals for $\vec{k}$ near the Brillouin-zone boundaries are changed the most. For other crystals the effects will be in general more significant.

APPENDIX A: CALCULATION OF $\phi_{ij}(\vec{q})$ AND T_{ij}

In Sec. V we gave the following alternative expressions for $\phi_{ij}(\vec{q})$ and T_{ij}:

$$\phi_{ij}(\vec{q}) = \sum_{\vec{\mu}} \sum_{m=1}^{d} \langle \phi_i(\vec{r}) | e^{2\pi i a^{-1} \vec{q} \cdot \vec{r}} | \phi_j(\vec{r} - a\vec{\mu} - a\vec{s}_m) \rangle$$

$$= a^{-3} \sum_{\vec{\nu}} S(\vec{\nu}) \phi_i^{*T}(\vec{q} + \vec{\nu}) \phi_j^T(-\vec{\nu}) , \tag{A1}$$

$$T_{ij} = \sum_{\vec{\mu}} \sum_{m=1}^{d} \langle \phi_i(\vec{r}) | -\tfrac{1}{2} \nabla^2 | \phi_j(\vec{r} - a\vec{\mu} - a\vec{s}_m) \rangle$$

$$= \frac{2\pi^2}{a^5} \sum_{t} g_t \nu_t^2 S(\vec{\nu}_t) \phi_i^{*T}(\vec{\nu}_t) \phi_j^T(-\vec{\nu}_t) . \tag{A2}$$

In this appendix we will summarize the specific forms of Eqs. (A1) and (A2) for the ϕ_i considered,

and we will discuss an analytical-summation method when STO's are used.

If the ϕ_i are $1s$ STO's with screening parameter ζ_i,

$$\phi_i^{1s}(\vec{r}) = (\zeta_i^3/\pi)^{1/2} e^{-\zeta_i r} , \qquad (A3)$$

and Eqs. (A1) and (A2) take the form

$$\phi_{ij}^{(1)}(\vec{q}) = \frac{8}{\pi^2} \sum_{\vec{v}} \frac{(\delta_i \delta_j)^{5/2} S(\vec{v})}{(|\vec{q} + \vec{v}|^2 + \delta_i^2)^2 (q^2 + \delta_j^2)^2} , \qquad (A4)$$

$$T_{ij}^{(1)} = \frac{16}{a^2} \sum_t g_t v_t^2 \frac{(\delta_i \delta_j)^{5/2} S(\vec{v})}{(v_t^2 + \delta_i^2)^2 (v_t^2 + \delta_j^2)^2} , \qquad (A5)$$

with $\delta_i = \zeta_i a/2\pi$.

A $5g$ STO can be written in the form

$$\phi_i^{5g}(\vec{r}) = \frac{(2\zeta_i)^{11/2}}{(10!)^{1/2}} r^4 e^{-\zeta_i r} T_2(\Omega)$$

$$+ \text{less-symmetric terms}, \qquad (A6)$$

where T_2 is the normalized cubic harmonic with $l = 4$. The less-symmetric terms in Eq. (A6) vanish when the Fourier transform of ϕ_i^{5g} is introduced in the cubic-lattice summations of Eqs. (A1) and (A2), and it therefore suffices to give the Fourier transform of the totally symmetric part. The appropriate ϕ_{ij} and T_{ij} between $1s$ and $5g$ STO's can then be obtained, using

$$(\phi_i^{5g})^T(\vec{q}) = \frac{2^8}{\pi} \left(\frac{a^3}{3}\right)^{1/2} \delta_i^{13/2} \frac{q^4 T_2(\Omega_q)}{(q^2 + \delta_i^2)^6} . \qquad (A7)$$

Next we consider the formulas for Eqs. (A1) and (A2) when "cutoff" $1s$ STO's are employed. These orbitals $\phi_i^{(2)}$ have $1s$ STO character inside the WS cells about the lattice points at which they are centered, and vanish outside,

$$\phi_i^{(2)}(\vec{r}) = (\zeta_i^3/\pi)^{1/2} e^{-\zeta_i r}, \quad \vec{r} \text{ inside WS cell}$$

$$= 0, \qquad\qquad \vec{r} \text{ outside WS cell}. \quad (A8)$$

Because of the definition of $\phi_i^{(2)}$, only the terms with $\vec{\mu} = 0$, $m = 1$ survive in the first expression for ϕ_{ij}. Thus

$$\phi_{ij}^{(2)}(\vec{q}) = (\zeta_i \zeta_j/\pi^2)^{3/2} [e^{-(\zeta_i + \zeta_j)r}]_{WS}^T(\vec{q}) , \qquad (A9)$$

where $[\ ]_{WS}^T$ indicates that the transform integration is to be taken over the WS cell only.

We considered the cutoff functions for the simple-cubic crystal. Its WS cell is a cube. In order to evaluate Eq. (A9), we write[25]

$$e^{-\zeta r} = (\zeta/\pi^{1/2}) \int_0^\infty \exp[-\tfrac{1}{4}\zeta^2 t^2 - (x^2 + y^2 + z^2)/t^2] dt . \qquad (A10)$$

Since the integrations in Eq. (A9) are for $-\tfrac{1}{2}a \le x \le \tfrac{1}{2}a$; $-\tfrac{1}{2}a \le y \le \tfrac{1}{2}a$; $-\tfrac{1}{2}a \le z \le \tfrac{1}{2}a$, Eq. (A10) enables independent integration over x, y, and z. If we define

$$F(v, w) = \int_0^{1/2} e^{-wx^2} \cos 2\pi wx\, dx , \qquad (A11)$$

Eq. (A9) reduces to

$$\phi_{ij}^{(2)}(\vec{q}) = 128\pi^{3/2} \zeta_{ij} (\delta_i \delta_j)^{3/2} \int_0^\infty dt\, e^{-\zeta_{ij}^2 t^2} t^2 \prod_{n=1}^3 F(t^{-2}, q_n) , \qquad (A12)$$

where $\zeta_{ij} = \tfrac{1}{2} a(\zeta_i + \zeta_j)$ and q_n is the nth Cartesian component of $\vec{q}$. The integrations in Eqs. (A11) and (A12) are done numerically using Simpson's rule. The $F(t^{-2}, q_n)$ values are computed for specified t and q_n values and stored as a matrix. Since the $\vec{q}$ vectors are reciprocal-lattice vectors (in units $2\pi/a$), the q_n are integers. Therefore the computation of the $\phi_{ij}^{(2)}$ for the different $\vec{q}$ requires reference to that single F matrix only. Consequently it only takes a few seconds on a Univac 1108 to calculate $\phi_{ij}^{(2)}$ for 150 star vectors to five significant figures.

Turning now to the evaluation of $T_{ij}^{(2)}$, we note that the definition in Eq. (A8) introduces into Eq. (A2) a discontinuity in the gradient of the lattice periodic factor at the WS cell boundaries. Therefore Eq. (A2) should be written[26]

$$T_{ij}^{(2)} = \tfrac{1}{2} \langle \vec{\nabla}\phi_i^{(2)}(\vec{r}) | \vec{\nabla}\phi_j^{(2)}(\vec{r}) \rangle_{WS} = \tfrac{1}{2}\zeta_i\zeta_j\phi_{ij}^{(2)}(0) . \qquad (A13)$$

Finally, we describe an analytical-summation method for the calculation of $\phi_{ij}^{(1)}$ and $T_{ij}^{(1)}$. Equations (A1) and (A2) involve three infinite summations. Though the convergence is satisfactory, the computation time involved is appreciable. In fact, their calculation takes most of the time preparatory to the Hartree–Fock iterations. We found that one summation could be performed analytically. It has been our experience that the remaining summations converge much faster. A similar situation was found with the crystal summations in I.

We will exemplify the algebraic process by deriving $\phi_{ij}^{(1)}$ for a sc lattice. This quantity can be cast in the form

$$\phi_{ij}^{(1)}(\vec{q}) = \frac{8}{\pi^2} (\delta_i \delta_j)^{5/2}$$

$$\times \sum_{u,v=-\infty}^{+\infty} \sum_{w=-\infty}^{+\infty} \frac{1}{(w^2 + \alpha^2)^2 [(w - z)^2 + \beta^2]^2} , \qquad (A14)$$

where

$$\alpha^2 = u^2 + v^2 + \delta_i^2 ;$$
$$\beta^2 = (u - x)^2 + (v - y)^2 + \delta_j^2 , \qquad (A15)$$

and x, y, z are the components of $\vec{q}$. The inner summation can be written

$$\sum_{w=-\infty}^{+\infty} \frac{1}{(w^2 + \alpha^2)^2 [(w - z)^2 + \beta^2]^2}$$

$$= \left(-\frac{1}{2\alpha} \frac{\partial}{\partial\alpha}\right) \left(-\frac{1}{2\beta} \frac{\partial}{\partial\beta}\right) S(\alpha, \beta, z) , \qquad (A16)$$

$$S(\alpha, \beta, z) = \sum_{w=-\infty}^{+\infty} \frac{1}{(w^2 + \alpha^2)[(w - z)^2 + \beta^2]} . \qquad (A17)$$

Now the sum in Eq. (A17) can be evaluated analytically by the residue method[27]:

$$S(\alpha, \beta, z) = \frac{\pi}{A^2 + 4\alpha^2 z^2} \left(B \frac{\coth\pi\beta}{\beta} - A \frac{\coth\pi\alpha}{\alpha} \right.$$

$$\left. + z \sin 2\pi z \, \mathrm{csch}^2 \pi\beta \right) \quad \text{(A18)}$$

with

$$A = \alpha^2 - \beta^2 - z^2 \; ; \quad B = \alpha^2 - \beta^2 + z^2 \; . \quad \text{(A19)}$$

Since in our case z is always an integer, the last term in Eq. (A18) vanishes. When $\alpha = \beta$, and $z = 0$, we have a special case with result

$$S(\alpha, \alpha, 0) = \frac{\pi}{2\alpha^3} \coth\pi\alpha + \frac{\pi^2}{2\alpha^2} \mathrm{csch}^2\pi\alpha \; . \quad \text{(A20)}$$

The working expression for $\phi_{ij}^{(1)}(\vec{q})$ can now be obtained easily by straightforward, though tedious, algebra.

The numerical benefits we obtained are quite considerable. To obtain five significant figures for $\phi_{ij}^{(1)}$, the triple summation normally required (u, v, w) values from -10 to $+10$. However, when the w summation is performed analytically, the same accuracy is obtained from a range of u and v values between -5 and $+5$. This causes a great reduction in computation time; on a Univac 1108 the triple-summation method for $\phi_{ij}^{(1)}$ takes about 210 sec for 143 star vectors $\vec{q}$ per ij pair. The analytical method reduces this time to about 12 sec.

We do not, however, expect many numerical advantages with the analytical method when higher STO's are used. In that case higher derivatives of $S(\alpha, \beta, z)$ will be needed, and this leads to very clumsy expressions. These complications probably offset the advantage of better convergence of the remaining double sum.

Using the technique described above, we derived formulas for $T_{ij}^{(1)}$ and $\phi_{ij}^{(1)}(\vec{q}_\nu)$ for all cubic structures considered. These are available on request.

APPENDIX B: $Q_{mn}^t(\vec{k})$ FOR SMALL STAR VECTORS

The major numerical effort for the exchange-energy contributions to the matrix consists of the calculation of the quantities $Q_{mn}^t(\vec{k})$ [Eq. (41)] for the star vectors $\vec{\nu} = 0$ and $\vec{\nu} = (1, 0, 0)$. In Eq. (62) we reduced their evaluation to an analytical calculation of the integrals

$$I_{pL}(\overline{\omega}) = \int_0^{\overline{\omega}} \omega^{p+1} Q_L \left[\frac{(1 + \omega^2)}{2\omega} \right] d\omega \; , \quad \text{(B1)}$$

with $\overline{\omega} = \overline{k}(\Omega_{k'})/|\vec{\nu} + \vec{k}|$, followed by a numerical integration over $\Omega_{k'}$. Here we will describe how the I_{pL} are calculated, and how the $\Omega_{k'}$ integration is performed.

In order to derive recurrence relations for the I_{pL}, we use

$$(L+1)Q_{L+1}(x) - (2L+1)xQ_L(x) + LQ_{L-1}(x) = 0 \; , \quad \text{(B2)}$$

$$\frac{d}{dx}[Q_{L+1}(x) - Q_{L-1}(x)] = (2L+1)Q_L(x) \; , \quad \text{(B3)}$$

$$Q_{L+1}(x) - Q_{L-1}(x) = (2L+1)q_L(x) \; , \quad \text{(B4)}$$

$$q_L(x) = (x^2 - 1)^{1/2} Q_L'(x) \; . \quad \text{(B5)}$$

Applying Eq. (B2), we derive

$$(L+1)I_{p,L+1} + LI_{p,L-1} - (L + \tfrac{1}{2})(I_{p+1,L} + I_{p-1,L}) = 0 \; . \quad \text{(B6)}$$

Let $z = (1 + \omega^2)/2\omega$; then $dz = \tfrac{1}{2}(1 - \omega^{-2}) d\omega$. Application of Eqs. (B2) and (B3) leads to

$$\tfrac{1}{2}(I_{p+1,L} - I_{p-1,L}) = \int_{\omega=0}^{\omega=\overline{\omega}} \omega^{p+2} Q_L(z) \, dz$$

$$= \frac{1}{(2L+1)} \int_{\omega=0}^{\omega=\overline{\omega}} \omega^{p+2} \left(\frac{d}{dz}[Q_{L+1}(z)\right.$$

$$\left. - Q_{L-1}(z)]\right) \left(\frac{dz}{d\omega}\right) d\omega$$

or

$$(L + \tfrac{1}{2})(I_{p+1,L} - I_{p-1,L}) + (p+2)(I_{p,L+1} - I_{p,L-1})$$

$$= \overline{\omega}^{p+2}[Q_{L+1}(\overline{z}) - Q_{L-1}(\overline{z})] \; , \quad \text{(B7)}$$

with $\overline{z} = (1 + \overline{\omega}^2)/2\overline{\omega}$. Adding and subtracting Eqs. (B6) and (B7), we finally have

$$-(2L+1)I_{p-1,L} + (p+L+3)I_{p,L+1} - (p-L+2)I_{p,L-1}$$

$$= \overline{\omega}^{p+2}[Q_{L+1}(\overline{z}) - Q_{L-1}(\overline{z})] \; , \quad \text{(B8)}$$

$$(2L+1)I_{p+1,L} + (p-L+1)I_{p,L+1} - (p+L+2)I_{p,L-1}$$

$$= \overline{\omega}^{p+2}[Q_{L+1}(\overline{z}) - Q_{L-1}(\overline{z})] \; . \quad \text{(B9)}$$

In all these equations, the argument of $I_{p,L}$ is $\overline{\omega}$.

Starting with values for I_{00} and $I_{-1,1}$, and repeated use of Eqs. (B8) and (B9), we can generate all I_{pL}. I_{00} and $I_{-1,1}$ are given by

$$I_{00}(\overline{\omega}) = \tfrac{2}{3}[Q_2(\overline{\omega}) - Q_0(\overline{\omega})] + 2\overline{\omega} \; , \quad \text{(B10)}$$

$$I_{-1,1}(\overline{\omega}) = \tfrac{1}{2}I_{00}(\overline{\omega}) - \overline{\omega} + \Lambda(\overline{\omega}) \; , \quad \text{(B11)}$$

$$\Lambda(\overline{\omega}) = \frac{1}{2}\int_0^{\overline{\omega}} \frac{dt}{t} \ln\left|\frac{1+t}{1-t}\right| = \sum_{j=0}^\infty \frac{\overline{\omega}^{2j+1}}{(2j+1)^2} \; , \quad \overline{\omega} \leq 1$$

$$= \frac{\pi^2}{4} - \sum_{j=0}^\infty \frac{\overline{\omega}^{-2j-1}}{(2j+1)^2} \; , \quad \overline{\omega} \geq 1 \; . \quad \text{(B12)}$$

The evaluation of $\Lambda(x)$ for $x \approx 1$ is troublesome because of the slow convergence of the sum in Eq. (B12). We note that $d\Lambda(x)/dx$ approaches infinity as x approaches 1. This behavior should be properly reproduced in any algebraic representation for $\Lambda(x)$. After some numerical experimentation, we decided to use the following set of expressions:

$$\frac{\Lambda(x)}{x} = \left(1 + \sum_{i=1}^{5} a_i x^{2i}\right) \bigg/ \left(1 + \sum_{j=1}^{5} b_j x^{2j}\right), \quad 0 \le x \le 0.97 \tag{B13}$$

$$a_1 = -2.197727, \quad b_1 = -2.308838,$$

$$a_2 = 1.673117, \quad b_2 = 1.889655,$$

$$a_3 = -0.5149340, \quad b_3 = -0.6529503,$$

$$a_4 = 0.05541671, \quad b_4 = 0.08715404,$$

$$a_5 = -0.0010380, \quad b_5 = -0.002928433,$$

$$\frac{\Lambda(x)}{x} = 0.8152765[1 - (1 - x^2)^{0.82}] + 0.4196336,$$
$$0.97 \le x \le 0.99 \tag{B14a}$$

$$\frac{\Lambda(x)}{x} = 0.9006413[1 - (1 - x^2)^{0.855}] + 0.3330597,$$
$$0.990 \le x \le 0.995 \tag{B14b}$$

$$\frac{\Lambda(x)}{x} = 0.9649497[1 - (1 - x^2)^{0.87}] + 0.2687513,$$
$$0.995 \le x \le 1.000 \tag{B14c}$$

Equation (B13) is an $[N, N]$ Padé approximant. The use of powers of $(1 - x^2)$ less than 1 assures the above-mentioned singularity in $d\Lambda(x)/dx$. The relative errors in Eqs. (B13) and (B14) are about 5×10^{-5}.

It follows from Eqs. (B8)–(B10) that the Q_L always appear in the combination $[Q_{L+1} - Q_{L-1}]$. $Q_L(x)$ approaches $+\infty$ for $x \to 1+$, but $[Q_{L+1} - Q_{L-1}]$ remains infinite. We therefore calculate directly the differences $Q_{L+1} - Q_{L-1}$, which are, according to Eq. (B4), proportional to the quantities designated q_L. The q_L satisfy a recurrence relation like

(B2). The starting values are

$$q_0(x) = -1 ;$$

$$q_1(x) = \tfrac{1}{2}(x^2 - 1)\ln\left|\frac{1+x}{1-x}\right| - x . \tag{B15}$$

For $x = 1$ we have a special case for which $q_1(1) = -1$. For $x \gtrsim 1.5$, Eq. (B2) is numerically unsatisfactory. In each recurrence step we lose several significant figures. Instead we used a downward-recurrence relation. If we define

$$r_L(x) = q_{L+1}(x)/q_L(x) \tag{B16}$$

then, using Eq. (B2), we have the downward-recurrence formula

$$r_{L-1}(x) = \frac{L+1}{(2L+1)x - Lr_L(x)} . \tag{B17}$$

From Eq. (B16) and the asymptotic behavior of $Q_L(x)$ for $L \gg x$, we find

$$r_L(x) \approx \frac{L+2}{(2L+3)x}, \quad L \gg x . \tag{B18}$$

By starting with $L = 50$, we found that $Q_{L+1} - Q_{L-1}$ for the L values we needed could be calculated in this way with six significant figures.

This concludes the specification of the computational scheme for the $I_{pL}(\overline{\omega})$. In the case of cubic symmetry we only need I_{pL} for even p and L, and it is therefore numerically advantageous to deduce recurrence relations from Eqs. (B8) and (B9) that involve $I_{2m,2n}(\overline{\omega})$ only $(m, n = 0, 1, 2, \ldots)$. Below we summarize the working relations we found satisfactory (the Q_L have argument $\overline{z}$):

$$I_{2n+2,2n+2} - I_{2n,2n} = \overline{\omega}^{2n+2} q_{2n+1} + \overline{\omega}^{2n+3} q_{2n+2} , \tag{B19}$$

$$(4n+2)(4n+4)I_{2n,2n+2} - (4n+1)(4n+3)I_{2n-2,2n} - (8n+5)I_{2n,2n} = 4n(4n+3)\overline{\omega}^{2n+1}q_{2n} + (4n+2)(4n+3)\overline{\omega}^{2n+2}q_{2n+1} , \tag{B20}$$

$$(2m+1)(2m-2n+3)(2m+2n+4)I_{2m+2,2n} - [4(2m+1)(2m+2)(2m+3) - (2m+1)(2m+2n+3)(2m+2n+4)$$
$$- (2m+3)(2m-2n)(2m-2n+1)]I_{2m,2n} + (2m+3)(2m-2n)(2m+2n+1)I_{2m-2,2n}$$
$$= 4(2m+1)(2m+3)(2n+2)\overline{\omega}^{2m+2}q_{2n+1} - 4n[(2m+1)(2m+2n+4)\overline{\omega}^2 + (2m-2n)(2m+3)]\overline{\omega}^{2m+1}q_{2n} . \tag{B21}$$

We replaced the angular integration in Eq. (62) by a weighted sum over integrand values for M independent star directions Ω_t. If $g(\Omega)$ were the function to be angularly integrated, then we write

$$\int g(\Omega) d\Omega = \sum_{t=1}^{M} w_t g(\Omega_t) , \tag{B22}$$

where the sum is over independent star directions. The w_t are determined from the requirement that Eq. (B22) be exact if $g(\Omega)$ were a linear combination of the M lowest-order cubic harmonics T_u. This implies the equations

$$\int T_u(\Omega) d\Omega = \sum_{t=1}^{M} w_t T_u(\Omega_t) = (4\pi)^{1/2} \delta_{u1}$$

$$(u = 1, 2, \ldots, M) . \tag{B23}$$

The w_t are easily determined from Eq. (B23) once M and the independent star directions Ω_t have been decided on. In our calculations we used $M = 7$, which means that Eq. (B22) is exact up to a cubic harmonic of order 12. Since we found nearly spherical Fermi surfaces, this integration scheme was found to be sufficiently accurate.

APPENDIX C: EXCHANGE POTENTIAL

The exchange operator in the Hartree–Fock method is intrinsically nonlocal, but if it is assumed that the functions $|\vec{k}\rangle$ are already known, it is possible to describe the effect of the exchange operator on $|\vec{k}\rangle$ by a $\vec{k}$-dependent multiplicative operator.

If we write the Hartree–Fock equation in operator form,

$$F|\vec{k}\rangle = \epsilon(\vec{k})|\vec{k}\rangle , \tag{C1}$$

and introduce the notation

$$|\vec{k}\rangle = e^{2\pi i a^{-1}\vec{k}\cdot\vec{r}}u(\vec{k},\vec{r}) , \tag{C2}$$

we have

$$F = -\tfrac{1}{2}\nabla^2 + C + X , \tag{C3}$$

where C and X are, respectively, the Coulomb and exchange operators,

$$C(\vec{r}) = (2/d)\int d\vec{r}' \int d\vec{k}' \, |u(\vec{k}',\vec{r}')|^2 h(\vec{r},\vec{r}') , \tag{C4}$$

$$X|\vec{k}\rangle = -\frac{e^{2\pi i a^{-1}\vec{k}\cdot\vec{r}}}{d}\int d\vec{r}' \int d\vec{k}' \, u^*(\vec{k}',\vec{r}')$$

$$\times \exp[2\pi i a^{-1}(\vec{k}-\vec{k}')\cdot(\vec{r}'-\vec{r})] \, \frac{u(\vec{k},\vec{r}')u(\vec{k}',\vec{r})}{|\vec{r}-\vec{r}'|} . \tag{C5}$$

An effective-exchange potential for operation on $|\vec{k}\rangle$ may now be defined as

$$V_x(\vec{k},\vec{r}) = X|\vec{k}\rangle/|\vec{k}\rangle . \tag{C6}$$

Owing to the nonlocal nature of X, V_x will in general be complex and dependent upon $\vec{k}$. By angular averaging, we may obtain a real-valued approximation to V_x which will be more convenient for comparison with approximate exchange potentials:

$$V_x \rightarrow V_x(k,\vec{r}) \equiv \langle V_x(\vec{k},\vec{r})\rangle_{\Omega_k} . \tag{C7}$$

A further averaging over occupied k values would lead to a local approximate potential.

Numerically we can proceed in two ways to calculate $V_x(k,\vec{r})$. We may make a direct evaluation, starting from Eq. (C6),

$$V_x^1(k,\vec{r}) = \left\langle X|\vec{k}\rangle/|\vec{k}\rangle \right\rangle_{\Omega_k} , \tag{C8}$$

or we may avoid the explicit use of the operator X by using the Hartree–Fock equation, thereby obtaining

$$V_x^2(k,\vec{r}) = \left\langle \epsilon(\vec{k}) - \frac{-\tfrac{1}{2}\nabla^2|\vec{k}\rangle}{|\vec{k}\rangle} - C(\vec{r}) \right\rangle_{\Omega_k} . \tag{C9}$$

The quantities V_x^1 and V_x^2 would be identical if the Hartree–Fock equation were exactly satisfied for all $\vec{r}$. As shown in the main text, a comparison of these quantities can yield an indication of the exactness of our solutions to the Hartree–Fock equations.

The expression for V_x^1 can be readily evaluated; we proceed here for the case that $u(\vec{k},\vec{r})$ is based on a single STO per lattice site and is therefore actually independent of $\vec{k}$, and that the Fermi surface is spherical. We then have $u(\vec{k},\vec{r}) = \sum_{\vec{\mu}}\Phi_1(\vec{r}-a\vec{\mu})$, and using the techniques described in Secs. III and IV, we obtain

$$V_x^1(k,\vec{r}) = -\frac{4k_F}{ad}\sum_{\vec{v}} S(\vec{v}) \frac{\phi_{11}(\vec{v})}{\phi_{11}(0)} \cos(2\pi a^{-1}\vec{v}\cdot\vec{r})$$

$$\times \left\langle F\left(\left|\frac{\vec{v}+\vec{k}}{k_F}\right|\right)\right\rangle_{\Omega_k} , \tag{C10}$$

where $S(\vec{v})$ and ϕ_{11} are defined in Eqs. (23) and (32), k_F is the Fermi radius in units $2\pi/a$, and

$$F(\eta) = \frac{1}{2} + \frac{1-\eta^2}{4\eta}\ln\left|\frac{1+\eta}{1-\eta}\right| . \tag{C11}$$

A parallel analysis on V_x^2 leads to the result

$$V_x^2(k,\vec{r}) = \epsilon(k) - \frac{2\pi^2}{a^2}k^2 + \frac{1}{2}\left\langle\frac{\nabla^2 u(\vec{k}\cdot\vec{r})}{u(\vec{k},\vec{r})}\right\rangle_{\Omega_k}$$

$$+ \frac{1}{\pi a}\sum_{\vec{v}}' v^{-2}S(\vec{v})e^{-2\pi i a^{-1}\vec{v}\cdot\vec{r}}\frac{\phi_{11}(\vec{v})}{\phi_{11}(0)}$$

$$- \frac{1}{\pi a}\sum_{\vec{v}}' v^{-2}S(\vec{v})e^{-2\pi i a^{-1}\vec{v}\cdot\vec{r}} . \tag{C12}$$

The term in Eq. (C12) involving $\nabla^2 u(\vec{k},\vec{r})$ may be evaluated by noting that $u(\vec{k},\vec{r})$ is a linear combination of STO's ϕ_1 of screening parameter ζ_1, and that $-\tfrac{1}{2}\nabla^2\phi_1(\vec{r}) = (\zeta_1/r - \tfrac{1}{2}\zeta_1^2)\phi_1(\vec{r})$. The last term in Eq. (C12) is most efficiently evaluated by performing the summation analytically in one of the three dimensions, using the formulas

$$\sum_{w=-\infty}^{\infty} \frac{\cos\gamma w}{w^2+\alpha^2} = \pi\frac{\cosh[\alpha(\pi-\gamma)]}{\alpha\sinh\pi\alpha} , \tag{C13}$$

$$\sum_{w=1}^{\infty} \cos\gamma w/w^2 = \tfrac{1}{12}\pi^2 - \tfrac{1}{2}\pi\gamma + \tfrac{1}{4}\gamma^2 , \tag{C14}$$

$$\sum_{w=-\infty}^{\infty} (-)^w \frac{\cos\gamma w}{w^2+\alpha^2} = \pi\frac{\cosh\alpha\gamma}{\alpha\sinh\pi\alpha} . \tag{C15}$$

We thus obtained the following expression for the bcc case:

$$\frac{1}{2}\sum_{\vec{v}}' S(\vec{v})e^{2\pi i a^{-1}\vec{v}\cdot\vec{r}} = \tfrac{1}{2}\gamma^2 + \tfrac{1}{2}(\gamma-\pi)^2 - \tfrac{1}{3}\pi^2$$

$$+ \pi\sum_{u,v\neq 0,0} \cos 2\pi i a^{-1}ux\cos 2\pi i a^{-1}vy$$

$$\times\left(\frac{\cosh\alpha(\pi-\gamma)+(-1)^{u+v}\cos\alpha\gamma}{\alpha\sinh\pi\alpha}\right) , \tag{C16}$$

where x, y, and z are the Cartesian components of $\vec{r}$, and $\gamma = 2\pi z/a$, $\alpha = (u^2+v^2)^{1/2}$. As with the analytical summations developed in Appendix A, we observed considerably improved convergence in the remaining double summation.

*Research sponsored by the Air Force Office of Scientific Research, Office of Aerospace Research, USAF, under Grant No. AFOSR-71-1992A. The United States Government is authorized to reproduce and distribute reprints for governmental purposes notwithstanding any copyright notation hereon. Also supported in part by the National Science Foundation (under Grant No. GP-31373X).

[1] J. M. Ziman, *Principles of the Theory of Solids* (Cambridge U.P., Cambridge, England, 1965).

[2] A. M. Boring and E. C. Snow, in *Computational Methods in Band Theory,* edited by P. M. Marcus, J. F. Janak, and A. R. Williams (Plenum, New York, 1971), p. 495; see also related papers in the same volume.

[3] J. C. Slater, *Quantum Theory of Molecules and Solids* (McGraw-Hill, New York, 1965), Vol. 2.

[4] F. E. Harris and H. J. Monkhorst, Phys. Rev. Lett. **23,** 1026 (1969).

[5] F. E. Harris and H. J. Monkhorst, in Ref. 2, p. 517.

[6] F. E. Harris and H. J. Monkhorst, Phys. Rev. B **2,** 4400 (1970).

[7] F. E. Harris and H. J. Monkhorst, Solid State Commun. **9,** 1449 (1971); F. E. Harris, L. Kumar, and H. J. Monkhorst, Int. J. Quantum Chem. **5S,** 527 (1971).

[8] R. A. Bonham, J. L. Peacher, and H. L. Cox, Jr., J. Chem. Phys. **40,** 3083 (1964).

[9] F. E. Harris and H. J. Monkhorst, Int. J. Quantum Chem. **6,** 601 (1972).

[10] *Handbook of Mathematical Functions,* edited by M. Abramowitz and I. A. Stegun (U.S. GPO, Washington, D. C., 1964), Eq. 8.9.2.

[11] Reference 3, p. 204.

[12] E. Wigner and H. B. Huntington, J. Chem. Phys. **3,** 764 (1935).

[13] R. Kronig, J. de Boer, and J. Korringa, Physica (Utr.) **12,** 245 (1946).

[14] J. L. Calais, Ark. Fys. **29,** 255 (1965).

[15] T. Schneider, Solid State Commun. **7,** 875 (1969); N. W. Ashcroft, Phys. Rev. Lett. **21,** 1748 (1968).

[16] F. E. Harris, L. Kumar, and H. J. Monkhorst, J. Phys. (Paris) **33,** C3-99 (1972).

[17] K. A. Brueckner, Adv. Chem. Phys. **15,** 215 (1969).

[18] J. C. Slater, Phys. Rev. **81,** 385 (1951).

[19] R. Gaspar, Acta Phys. Hung. 3, 263 (1954).

[20] W. Kohn and L. J. Sham, Phys. Rev. **140,** A1133 (1965).

[21] J. C. Slater, in Ref. 2, p. 447; Int. J. Quantum Chem. **4S,** 3 (1970); Int. J. Quantum Chem. **5S,** 403 (1971).

[22] K. H. Johnson and F. C. Smith, Jr., Int. J. Quantum Chem. **5S,** 429 (1971).

[23] P. Hohenberg and W. Kohn, Phys. Rev. **136,** B864 (1964).

[24] D. A. Liberman, Phys. Rev. **171,** 1 (1968).

[25] I. Shavitt and M. Karplus, J. Chem. Phys. **43,** 398 (1965).

[26] Reference 3, Appendix 6.

[27] D. S. Mitrinović, *Calculus of Residues* (Noordhoff, Groningen, 1966).